Physics – Uspekhi **66** (7) 673 – 690 (2023)

REVIEWS OF TOPICAL PROBLEMS

PACS numbers: **61.43. – j**, 61.72.J – , 81.05.Kf

A novel view of the nature of formation of metallic glasses, their structural relaxation, and crystallization

N P Kobelev, V A Khonik

DOI: https://doi.org/10.3367/UFNe.2022.04.039173

Contents

Abstract. An alternative concept of the formation of the defect structure and properties of metallic glasses — the interstitialcy theory (IT), which has been actively developed recently — is systematically laid out. The premises and basic hypotheses of the IT are presented, and the experimental data pertaining to the assessment of its adequacy are considered. The multifaceted relation between the relaxation of the shear elasticity and heat phenomena upon various types of thermal processing of metallic glasses is analyzed in detail. A simple mathematical IT formalism is shown to provide a good description of experimental data. The most important result of the IT is an adequate description of the excess thermodynamic potentials of metallic glasses. Problems surrounding the IT and approaches to its further development are considered.

Keywords: metallic glasses, structural relaxation, crystallization, defects, interstitialcy theory

N P Kobelev [1, a], **V A Khonik** [2, b]
[1] Institute of Solid State Physics, Russian Academy of Sciences, ul. Akademika Osip'yana 2, 142432 Chernogolovka, Moscow region, Russian Federation
[2] Voronezh State Pedagogical University, ul. Lenina 86, 394043 Voronezh, Russian Federation
E-mail: [a] kobelev@issp.ac.ru, [b] v.a.khonik@yandex.ru

Received 2 March 2022, revised 21 March 2022
Uspekhi Fizicheskikh Nauk **193** (7) 717 – 736 (2023)
Translated by M Zh Shmatikov

1. Introduction

Intensive studies of metallic glasses (MGs), which began in the 1980s, continue to the present. Interest in MGs is due both to the apparent potential and success of their application, and to a number of still unsolved purely academic problems related to the nature of the structural state of MG, its relationship with their physical properties, glass transition kinetics, relaxation phenomena, and the response to external factors. It was initially expected that, since nondirectional metallic bonding dominates in MG, describing various physical phenomena would be a simpler task than, for example, in the case of oxide glasses with directional covalent bonds. This expectation, however, was not justified, and no generally accepted theoretical approach to these problems has been developed so far. This situation, on the one hand, is a strong motivation for further research, and, on the other hand, imposes certain restrictions on the solution to problems of an applied nature.

Metallic glasses are primarily prepared by quenching a melt, which in turn is the result of crystal melting. Therefore, a relationship should be expected between the properties of solid glass (i.e., frozen melt) and the original (parent) crystal.[1] Such a relationship should be reflected in an adequate theoretical/model approach to describing the properties of MG. On the other hand, the noncrystalline nature of the MG structure causes its spontaneous evolution towards a lower Gibbs potential, which is generally called 'structural relaxa-

[1] More precisely, here and below, the parent crystal means a polycrystalline structure that arises as a result of the complete crystallization of glass and does not undergo any subsequent phase transformations.

tion.' It is usually assumed that structural relaxation is realized through atomic rearrangements in some nanoregions, conventionally called 'defects.' Consequently, this approach should involve ideas about the evolution of a defective subsystem at all stages, from melting of the parent crystal and quenching of the melt to changes in glass properties during heat treatment and the effect of external factors.

At present, a large number of theoretical models have been proposed to describe the structure, its defects, and various properties of MGs (see, for example, [1–11]), which are used with varying degrees of success. A common problem of these models is the artificial definition of defects not related to the thermal history of glass, including its origin from the crystalline state, which is, moreover, the end point of its evolution [12]. This question is usually not even mentioned. Therefore, a connection of glass and its defects with the parent crystal cannot be established. However, attempts to establish a relationship between the dominant structural elements of glass and crystal have been made [13].

Perhaps the only theoretical model which is not typically plagued with this shortcoming is Granato's interstitialcy theory (IT) [14, 15]. The IT suggests that the melting of the parent crystal is associated with the generation of interstitial defects in the dumbbell configuration, which in the melt do not retain the geometric structure inherent in the crystal but are identifiable structural units that inherit the main properties of dumbbell interstitials. Defects such as interstitial dumbbells are 'frozen' into the structure of a solid MGs as a result of melt quenching. Various relaxation phenomena in MGs can then be interpreted as the result of changes in the defect subsystem of the interstitial dumbbells. These ideas have developed significantly in the last few years. It is shown, in particular, that exo- and endothermal phenomena during structural relaxation and crystallization of MGs can be described almost exactly on the basis of measurements of macroscopic shear elasticity, which, it would seem at first glance, has nothing in common with thermal phenomena at all. It has also been established that excess thermodynamic potentials (i.e., those due to the actual noncrystallinity of the structure), primarily excess internal energy and excess entropy, are at least by 85–90% related to the elastic energy of interstitial-type defects frozen in from the melt and its dissipation in heat under heating. On the whole, in terms of the quality, consistency, and breadth of interpretation of the experiments, the results obtained definitely distinguish IT from a number of other model concepts, owing to which, in our opinion, it is one of the most promising approaches to a holistic understanding of the nature of the formation, structural relaxation, and crystallization of MGs. These ideas are outlined in the present review.

2. Prerequisites for the emergence and main provisions of the interstitialcy theory

The basic component of the IT is the concept of interstitial atoms in a dumbbell configuration or interstitial dumbbells. Therefore, it is natural to begin a consistent presentation of the IT with some general remarks about interstitial defects.

Until the early 1970s, it was assumed that interstitial atoms occupy an octahedral cavity at the center of a face-centered cubic (fcc) cell (Fig. 1a). In the mid-1970s, it became clear that interstitial atoms in simple metals have a dumbbell (split) configuration (Fig. 1b). At present, it is generally

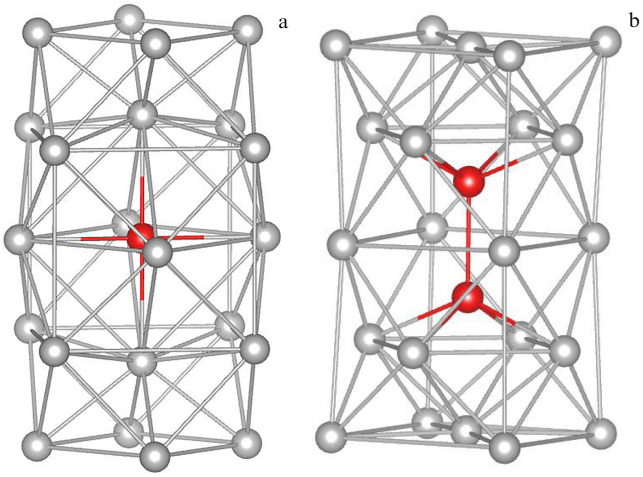

Figure 1. Interstitial atoms in (a) octahedral and (b) dumbbell (split) configurations in a computer model of an fcc lattice [16].

accepted that interstitial dumbbells exist in all main crystal structures and, moreover, usually have the lowest possible formation enthalpy [17–20].

However, the difference between interstitial atoms in the octahedral and dumbbell configurations is fundamental. An octahedral interstitial site, like a vacancy, has the same point symmetry group as the atoms of the lattice, as a result of which it does not interact with external shear stress. On the contrary, the point symmetry of the interstitial dumbbell atoms is lower than the symmetry of the lattice atoms; the dumbbell has a certain orientation (a dumbbell with the [001] orientation is shown in Fig. 1b) and is an elastic dipole, which therefore effectively interacts with the field of the external shear stress [21].

A significant contribution to the study of the properties of interstitial atoms was made by Granato et al. [22, 23], who irradiated Cu single crystals with thermal neutrons at a temperature $T = 4$ K with simultaneous measurements of all elastic moduli. Irradiation caused the formation of isolated Frenkel pairs, while the liquid-helium temperature ensured low mobility of interstitial atoms and prevented their annihilation with vacancies. It has been established, first, that all elastic moduli decrease during irradiation (with increasing defect concentration), but the shear modulus decreases much faster, as shown in Fig. 2. It was also found that interstitial defects are formed in a dumbbell configuration [22]. It is with the latter circumstance that a strong decrease in the shear modulus is associated (the so-called diaelastic effect). Granato also emphasized that the extrapolation of the shear modulus in Fig. 2 towards higher concentrations c gives a zero shear modulus at $c \approx 2-3\%$ [24]. As is known, a zero (or very small) shear modulus is a characteristic feature of a liquid [25]. The result obtained in [24] showed that, if 2–3% of interstitial dumbbells are somehow introduced into the crystal, the crystal should turn into a liquid.

Research carried out in the 1970s also established two other important properties of interstitial dumbbells. First, the unstable position of two atoms of the dumbbell core (Fig. 1b) causes the appearance of characteristic low-frequency (at frequencies several times lower than the Debye one) and high-frequency (above the Debye frequency) vibrational modes associated with in-phase and out-of-phase vibrations

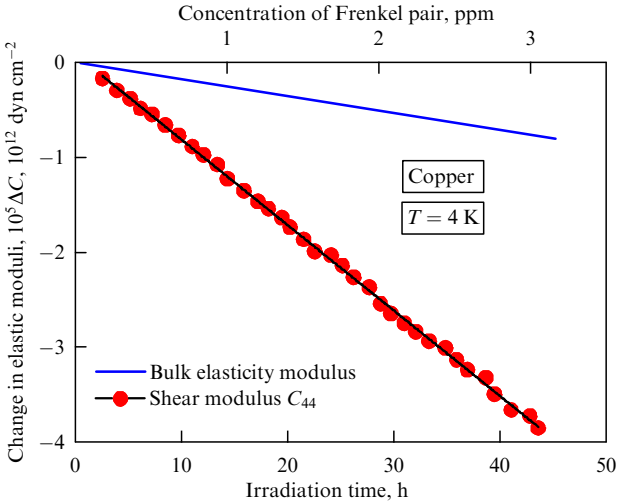

Figure 2. Effect of neutron irradiation on the high-frequency shear modulus and bulk modulus of a Cu single crystal [23].

of dumbbell atoms [26]. The low-frequency vibrational modes directly determine the high vibrational entropy component, the entropy of formation, which, according to estimates for copper, was $2 \leqslant S_i/k_B \leqslant 15$ (k_B is the Boltzmann constant) [15, 27], exceeding severalfold or even by an order of magnitude the corresponding value for vacancies [28] (according to [29], the entropy of vacancy formation can even be negative). The high formation entropy plays a crucial role in assessing the concentration of interstitial dumbbells. It is usually believed that, since the dumbbell formation enthalpy H_i is much greater than that for vacancies, the concentration of interstitial dumbbells should be negligible, and the this assertion can be found even in modern textbooks [30]. However, this argument does not take into account that the concentration of interstitial dumbbells is determined not by their formation enthalpy but by the Gibbs formation potential $\Phi_i = H_i - TS_i$, which decreases with temperature and, at a high formation entropy, can become comparable to or even less than that for vacancies. Consequently, the concentration of dumbbells can be very large and even exceed that of vacancies. This is all the more true since the formation enthalpy can decrease at high concentrations of dumbbells and, as a result, their concentration can increase like an avalanche, causing loss of shear stability and melting [15]. We return to the discussion of this situation in Section 3.

The foregoing enabled Granato to formulate the interstitialcy theory, published initially in [14] and later in a simplified version in [15]. An equation was derived for the excess Gibbs potential (with respect to a defect-free crystal) $\Delta\Phi$ depending on the concentration of interstitial dumbbells c_i and temperature, the material parameters being chosen for copper. It is shown that at temperatures below $0.85T_m$ (T_m is the melting point) there is only one $\Delta\Phi$ minimum corresponding to a low equilibrium concentration of dumbbells. In the interval $0.85T_m \leqslant T \leqslant T_m$, there are two $\Delta\Phi$ minima: a deep minimum at small c_i and a shallow minimum at large ones. The former is due to dumbbells in an equilibrium crystal, while the latter corresponds to interstitial-type defects, which remain identifiable objects in a metastable supercooled liquid [31]. At the melting point $T = T_m$, there are two equally deep $\Delta\Phi$ minima corresponding to thermodynamic equilibrium between a crystal with a low concentration c_i and a liquid with a high concentration c_i. In the interval $T_m \leqslant T \leqslant 1.15T_m$, a metastable superheated crystal and an equilibrium liquid can coexist at small and large c_i, respectively. Finally, at $T > 1.15T_m$, only an equilibrium liquid with a concentration c_i of several percent is thermodynamically stable. Thus, depending on the temperature and defect concentration c_i, the IT predicts the equilibrium and metastable states of the liquid and crystal. Recently performed similar calculations for aluminum yielded the same results [32].

Granato has shown that the enthalpy of formation of interstitial dumbbells H_i is proportional to the unrelaxed (high-frequency) shear modulus G and can be represented as

$$\frac{\partial H_i}{\partial c} = \alpha G\Omega\,, \tag{1}$$

where α is a dimensionless parameter of the order of unity, which, as it turned out later, is the second invariant of the elastic deformation field of the defect [33], and Ω is the volume per atom. Shear modulus G depends exponentially on the defect concentration $c_i = c$:

$$G = \mu \exp(-Bc)\,, \tag{2}$$

where μ is the shear modulus of the defect-free parent crystal, $B = \alpha\beta$, and parameter β is the dimensionless 'shear susceptibility.' According to Granato, $\beta = -3C_{4444}/C_{44} \approx 40$, where $C_{44} = \mu$ is the shear modulus of the crystal and C_{4444} is its fourth-order shear modulus (due to the anharmonicity of the interatomic interaction). On the other hand, the shear susceptibility is related to internal energy U of the crystal as $\beta = (1/16\mu)(\partial^4 U/\partial\varepsilon^4)$, where ε is the shear deformation. Thus, the shear susceptibility is proportional to the ratio of the shear modulus of the fourth rank to the 'ordinary' shear modulus and, in essence, is a fundamental parameter connecting the diaelastic effect (decrease in the shear modulus due to defects), the defect structure, and the anharmonicity of the interatomic interaction potential. As was established later, the shear susceptibility also determines thermal effects upon heating and varies for various MGs in a rather narrow range of $16 \leqslant \beta \leqslant 21$ [34], which is in principle consistent with the quoted Granato's estimate.

Simple equations (1) and (2) form the basis of the IT formalism. Although the IT contains a number of assumptions and approximations, and numerical calculations were performed for the case of simple metals, it gives a number of predictions that can be verified experimentally. Moreover, the consistent application of IT has made it possible to quantitatively interpret a number of phenomena in multicomponent MGs, as shown in Sections 3–12 (see also review [28] and the literature cited there).

3. Assessment of the adequacy of the basic hypotheses of the interstitialcy theory

The cornerstone of the IT is the concept of a rapid increase in the concentration of interstitial dumbbells when approaching the melting temperature T_m and the high entropy of their formation. These issues have been specifically investigated by means of precision measurements of the shear modulus of aluminum and indium at high temperatures, including premelting ones [35, 36]. A significant diaelastic effect was observed, which enhances with increasing temperature and indicates a rapid increase in the concentration of interstitial dumbbells. In approaching T_m, the dumbbell concentration

becomes comparable to the vacancy concentration in the case of Al and even significantly exceeds it for In. For Al, an estimate of the formation entropy $S_i/k_B \approx 22$ was obtained, in agreement with Granato's results [37]. However, as shown by a recent analysis, the formation entropy of point defects should be estimated taking into account the temperature dependence of the formation enthalpy, which in the case of Al leads to a decrease in the estimate of the formation entropy to $S_i/k_B \approx 7$ [29]. Nevertheless, even with such an estimate of S_i, it turns out that about 70% of the melting entropy Al observed in the experiment can be interpreted as the result of an avalanche-like generation of interstitial dumbbells at $T = T_m$ [32]. On the other hand, the high total entropy of dumbbells (including the vibrational and concentration parts), according to Granato, provides an explanation for the Richards rule asserting that the melting entropy of most elements of the periodic system is close to $1.2k_B$ per atom [38, 39]. We also note that simple metals exhibit a significant nonlinear increase in heat capacity in the region of pre-melting temperatures, for which there is currently no generally accepted explanation. As shown by the analysis performed on the example of aluminum, this increase can be due to the intense generation of interstitial dumbbells at temperatures close to T_m [40].

Another basic IT hypothesis is the assertion about the dominance of the shear energy U_{shear} in the total elastic energy of crystal and glass defects, which is directly reflected in Eqn (2). This statement goes back to studies of the 1950s–1960s, in which it was assumed that the change in the Gibbs potential of a defective crystal is proportional to the shear modulus G [41, 42]. On the other hand, according to [43],

$$\frac{U_{dil}}{U_{shear}} = \frac{2B/G}{9(B/G)^2 + 8B/G + 4} \leqslant 0.1\,, \qquad (3)$$

where B is the bulk modulus and U_{dil} is the dilatation component of the shear energy. However, formula (3), obtained in the linear theory of elasticity, does not take into account the energy of the defect core. To circumvent this difficulty, a molecular dynamics simulation of interstitial dumbbells in four fcc metals was carried out, which showed that in all cases the ratio U_{dil}/U_{shear} is approximately twice as large as that determined by Eqn (3), due to taking into account the elastic energy of the defect core [16]. Equation (3) with such a correction introduced was applied to interstitial dumbbells in 63 polycrystalline metals. The results obtained are shown in Fig. 3. As can be seen, the ratio U_{dil}/U_{shear} does not exceed 0.15 for more than 90% of the metals. Assuming that metallic glasses, in accordance with the IT, contain similar defects such as dumbbell interstitials, the same calculations were carried out for 189 MGs. Figure 3 shows that the result is very similar to that for the case of polycrystals, i.e., shear elastic energy dominates in all cases. The shear modulus should therefore be interpreted as the main macroscopic parameter for assessing the evolution kinetics of a defective subsystem.

Thus, the basic IT hypotheses, although they have been tested to a large extent only on simple metals, nevertheless correspond to experimental data.

4. Identification of 'interstitial defects' in glass

It is assumed in the IT that 'interstitial atoms' in a noncrystalline state behave in the same way as interstitial dumbbells in a crystal lattice. However, it is clear that the geometric definition of an interstitial defect as two atoms tending to occupy the same place in the crystal lattice (Fig. 1b) does not make sense for a noncrystalline structure. Granato proposed that the interstitial dumbbell by interpreted in this case as two atoms tending to occupy the same minimum of potential energy [44]. However, an appropriate algorithm to identify defects is difficult, if not impossible, to implement. Therefore, one of the methods for identifying an 'interstitial defect' is a comparison of its characteristics with the properties of an interstitial dumbbell in a crystal. This method was first implemented by the authors of [31], who showed that interstitials at their high concentration in a crystal demonstrate a cooperative string-like motion similar to that in a liquid. The string-like character of motion is one of the properties of atoms in an interstitial dumbbell in a crystal [46]. String-like motions of atoms in supercooled glasses and melts have been repeatedly described in the literature [9, 47–49]. It has been noted that such vibrational modes, similar to the motion of atoms in an interstitial dumbbell in a crystal [49–51], indirectly indicate their existence in supercooled liquids and glasses.

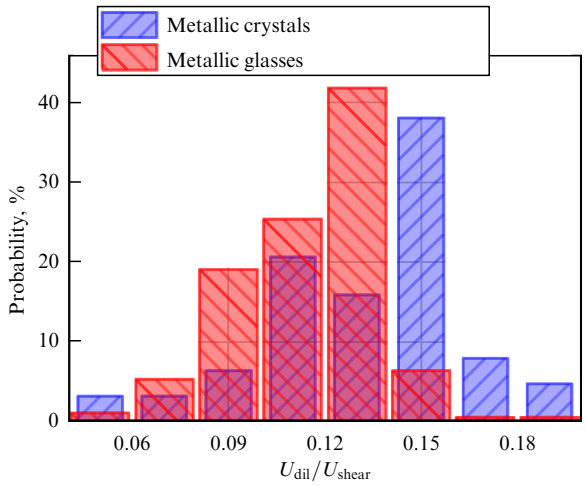

Figure 3. Distribution histograms of the dilation and shear energy ratio U_{dil}/U_{shear} of an interstitial dumbbell for 63 polycrystalline metals and similar defects for 189 metallic glasses [16].

As mentioned in Section 2, the introduction of interstitial dumbbells into a crystal results in the appearance of characteristic low-frequency and high-frequency modes in the vibrational spectrum. This circumstance can be used to indirectly identify the presence of such defects in the noncrystalline state. Figure 4 shows, as an example, the vibrational density of states (VDOS) of an fcc crystal of a high-entropy FeNiCrCoCu alloy, atoms of an interstitial dumbbell in it, and glasses of the same chemical composition [45]. Of greatest interest is the VDOS peak that arises for dumbbell atoms in the low-frequency region of 2 THz, which is absent in an ideal crystal. A comparison of the VDOS of a crystal and glass shows that the density of vibrational states of the noncrystalline structure is increased in the low-frequency region, which may be indirect confirmation of the presence of defects such as dumbbell interstitials in the glass. Detailed studies on noncrystalline aluminum confirm this assumption [45, 52]. It should be emphasized that the excess density of vibrational states in the low-frequency region is a universal feature of MGs [53].

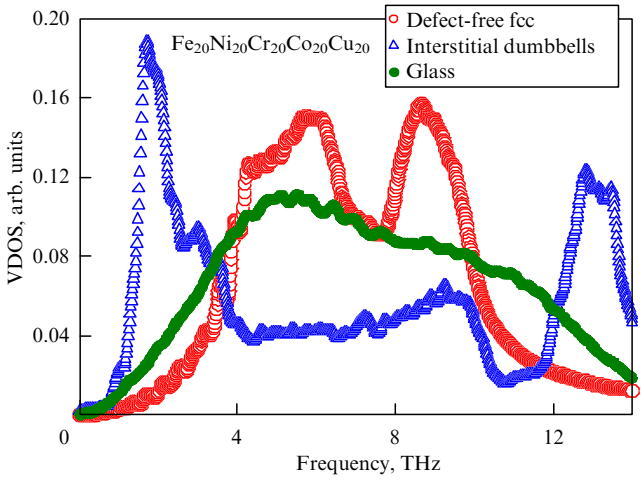

Figure 4. Densities of vibrational states of atoms in a defect-free crystal, a separate interstitial dumbbell, and glasslike $Fe_{20}Ni_{20}Cr_{20}Co_{20}Cu_{20}$ [45].

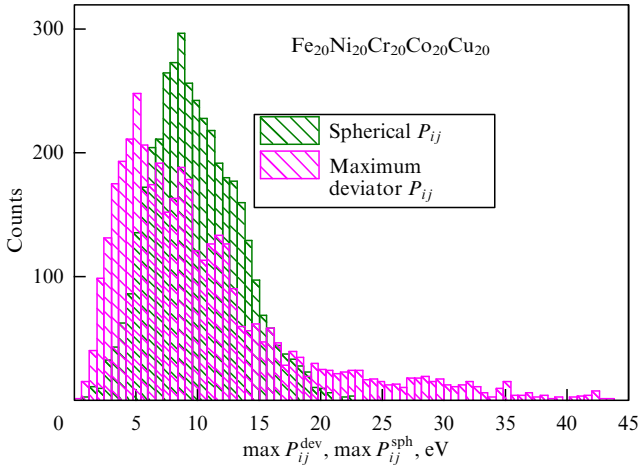

Figure 5. Distribution of spherical and maximum deviator components of dipole tensors P_{ij}^m in noncrystalline $Fe_{20}Ni_{20}Cr_{20}Co_{20}Cu_{20}$ [55].

Thus, the assumption about the presence in the glass structure of formations with properties similar to those of interstitial dumbbells seems to be quite justified. However, questions arise: in what specific way can localized defects of this type be isolated and identified in the glass structure and how can their size and structure be determined? One of the elements of a solution to this problem is the observation that, by its nature, an interstitial dumbbell is an elastic dipole, i.e., an atomic configuration with local symmetry lower than the symmetry of the surrounding matrix [21]. Such defects create local internal deformations, leading to an increase in internal stresses, interaction with the field of applied shear stresses, and a decrease in the effective shear modulus. It turns out that, using the expansion of the internal energy of a material with defects such as elastic dipoles in terms of the invariants of the elastic deformation fields ε_{ij} created by them, expressions can be derived that relate the accumulated internal energy and the change in elastic properties with the concentration of such defects [33, 54]. The structure of the formulas for the internal energy and the change in the shear modulus with the introduction of defects are highly similar to that of the basic formulas (1) and (2) of the IT. The physical meaning of the parameter α in Eqns (1) and (2) was also determined; it turned out to be related to the second invariant of the defect deformation field:

$$\alpha = \frac{\partial \int \varepsilon_{ij}\,\varepsilon_{ji}\,\mathrm{d}V}{V\,\partial c}\,,$$

where V is the volume of the material.

Based on the foregoing, an attempt can be made to identify defects in glass using the fact that they are elastic dipoles. A universal characteristic of elastic dipoles is the dipole tensor P_{ij}, which is defined as the derivative of the mechanical stress tensor σ_{ij} with respect to the number of defects per unit volume at constant strain [21]. In the case of a computer model of a crystal, dipole tensors can be calculated using an approximate formula as the difference between mechanical stresses in a crystal with defects and in an ideal crystal lattice. For a noncrystalline structure, the situation is much more complicated, since there is no correct definition of the 'ideal' (defect-free) state of glass. To circumvent this complexity, it was proposed to assign to each mth atom of

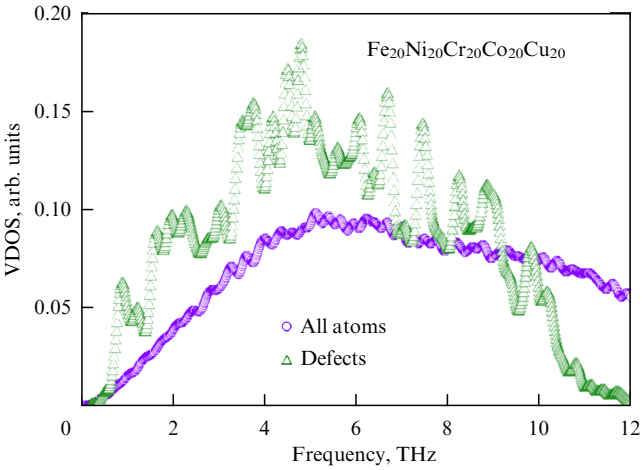

Figure 6. Spectra of the vibrational density of states in noncrystalline $Fe_{20}Ni_{20}Cr_{20}Co_{20}Cu_{20}$. Spectra are shown for the entire model and its defect subsystem [55].

the model a dipole tensor

$$P_{ij}^m = V(\sigma_{ij}^{Ng} - \sigma_{ij}^m)\,, \qquad (4)$$

where N is the number of atoms in the model structure, V is its volume, σ_{ij}^{Ng} is the stress tensor in the initial glass, and σ_{ij}^m is the stress tensor after removal of the mth atom in the unchanged V [55]. Thus, the initial state itself was used as the 'ideal' structure. The tensors P_{ij} calculated in this way were reduced to a diagonal form for further analysis and presented as the sum of the spherical and deviatoric components. An assessment of the adequacy of Eqn (4) showed that the dipole tensor of the interstitial dumbbell in a crystal, calculated using this formula, coincides with the estimate based on the standard relation [55]. The distribution of the spherical and deviatoric components of the dipole tensors of all atoms in noncrystalline FeNiCrCoCu is displayed in Fig. 5, which shows that for spherical components this distribution is close to normal, while the deviatoric component features a pronounced 'tail' in the region of large values of the dipole components. It is natural to assume that it is the atoms with large values of the deviatoric components that form the 'defect' glass subsystem. Figure 6 shows the vibrational densities of states in noncrystalline FeNiCrCoCu

for the entire model and its defect subsystem, which includes atoms with deviatoric components exceeding those at the end of the distribution of spherical components (see Fig. 5). As can be seen, atoms with large values of the deviatoric components are characterized by an increased density of states in the low-frequency region, which is typical of interstitial dumbbells. Moreover, the estimated concentration of such atoms almost coincided with the concentration of defects estimated using the Granato formula (2), i.e., $c = (1/\beta)\ln(\mu/G)$.

It is important to note that the application of shear deformation and the change of its sign alter the axes of the dipole tensors of most atoms of the defect subsystem. Such a reaction of a defective subsystem indicates that it can be considered a distributed network of elastic dipoles. The proposed method thus makes it possible to identify defect atoms in a model glass, and it can be considered a tool for a detailed analysis of the structure of MGs.

5. Thermal effects. Enthalpy relaxation kinetics

We now consider the application of the mathematical IT formalism for the analysis of various relaxation phenomena occurring during structural relaxation and crystallization of MGs.

Basic formula (2) of the IT shows that shear modulus G depends on concentration of defects c (both during structural relaxation and crystallization of MGs). In turn, formation enthalpy H_i, according to Eqn (1), depends on the shear modulus. Thus, a variation in the concentration of defects causes a change in the enthalpy of a substance as a result of a change in both the concentration of defects per se and the enthalpy of formation of a single defect. Therefore, a change in the concentration of defects, which can be tracked by measuring the shear moduli, leads to the appearance of thermal effects that can be detected calorimetrically. The concentration of defects can be excluded from the system of equations (1) and (2) and an expression for the heat flux $W = (1/m)(\delta Q/\delta t)$ can be derived, where Q is the heat of the process, m is the mass, t is time, in the form [28]

$$W = \frac{\dot{T}}{\rho\beta}\left(\frac{G}{\mu}\frac{\partial\mu}{\partial T} - \frac{\partial G}{\partial T}\right), \qquad (5)$$

where ρ is the density and $\dot{T}$ is the heating rate. As can be seen, the heat flux for a given MG at $\dot{T} = \text{const}$ is determined by shear moduli of the glass G and the parent crystal μ, as well as their derivatives with respect to temperature. Should high-precision data on the temperature dependences of $G(T)$ and $\mu(T)$ be available, Eqn (5) could be used to calculate heat flux W, which at the same time can be directly measured by differential scanning calorimetry (DSC) and compared with the calculation results.

A typical example of corresponding experimental data is presented in Figs 7 and 8. Figure 7 shows the temperature dependences of high-frequency shear modulus G, characteristic of Zr-based MG, in the initial state and after heating to 900 K, which causes complete crystallization. The initial state is characterized by an anharmonic decrease in G as the temperature is lowered to ≈ 500 K (dashed line), after which structural relaxation begins, causing some slowdown in the decrease in the modulus.[2] When the calorimetric glass

[2] Isothermal relaxation of the MG at $T < T_g$ causes a logarithmic increase in the shear modulus after a certain transition period, which is naturally explained in the IT [57].

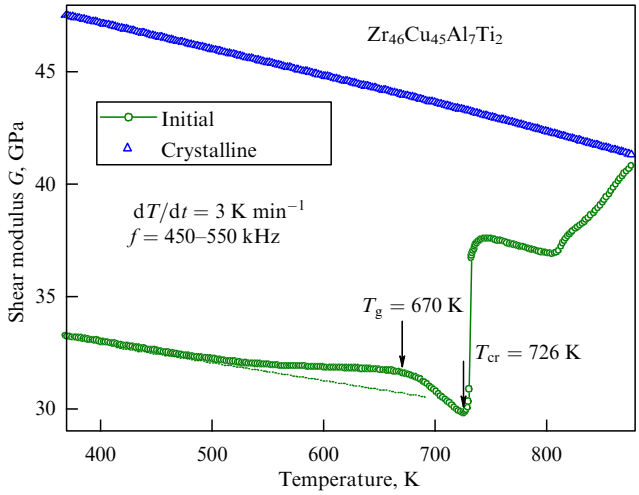

Figure 7. Temperature dependences of the shear modulus of metallic glass $Zr_{46}Cu_{45}Al_7Ti_2$ in the initial state and after complete crystallization. Arrows show the calorimetric temperature of glass transition T_g and the beginning of crystallization T_{cr} [56].

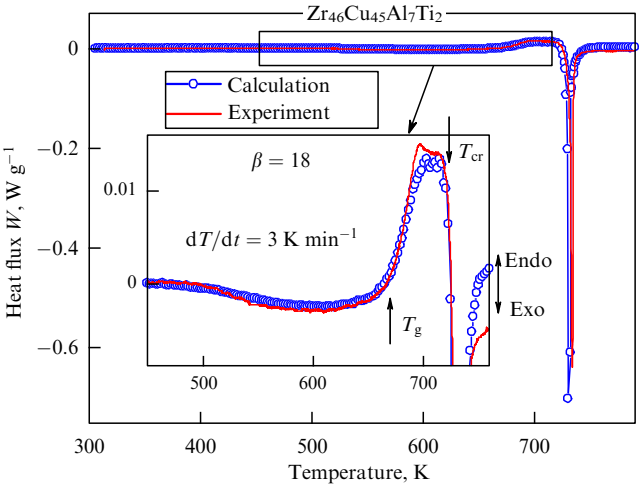

Figure 8. Experimental (solid red curve) and calculated (using Eqn (5)) (blue circles) thermograms of the DSC of $Zr_{46}Cu_{45}Al_7Ti_2$ MG. For the calculation, we used temperature dependences of the shear modulus in the initial state $G(T)$ and after complete crystallization $\mu(T)$ shown in Fig. 7 [56].

transition temperature $T_g \approx 670$ K is reached, G starts to decrease significantly up to the moment of the onset of crystallization at $T_{cr} \approx 726$ K. The shear modulus in the crystalline state μ smoothly, without any kinks, diminishes with decreasing temperature.

Figure 8 shows an experimental DSC (differential scanning calorimetry) thermogram of the same MG obtained at the same heating rate. It can be seen that structural relaxation at temperatures above ≈ 500 K is accompanied by an exothermic reaction, which, at a temperature close to 670 K, is replaced by a significant endothermal reaction, and this temperature, by definition, is taken as the calorimetric glass transition temperature T_g. The interval $T_g \leqslant T \leqslant T_{cr}$ corresponds to the state of a supercooled liquid, while, at $T > T_{cr}$, strong heat release due to crystallization begins.

The temperature dependences of shear moduli $G(T)$ and $\mu(T)$ shown in Fig. 7 were used to calculate the DSC

thermogram using formula (5), the result of which is shown by blue circles in Fig. 8. As can be seen, the calculation very well reproduces all thermal effects observed during MG heating: exothermic structural relaxation at $T < T_g$, endothermal reaction in the supercooled liquid state, and the exothermic crystallization reaction. The last circumstance is of particular interest, and we return to its discussion in Section 8.

In calculating temperature dependence $W(T)$ in Fig. 8, we used the values of shear susceptibility β obtained in other experiments from a comparison of the temperature dependences of the shear modulus and the heat flux in the initial and relaxed samples [28]. Moreover, it turns out that β can also be determined from completely independent experiments. As mentioned in Section 2, shear susceptibility β is equal to the ratio of the fourth-order shear modulus to the 'ordinary' shear modulus (i.e., the second-order shear modulus) [14]. The calculations of fourth-order moduli based on ultrasonic measurements for three MGs showed that the β values determined in this way range from 16 to 21, exactly the same as for the β values obtained using measurements of the shear modulus and heat flux [58]. We also note that the shear susceptibility β for a specific MG is usually determined with an accuracy of no worse than 10–15% [28]. It should be especially emphasized that Eqn (5) contains no fitting parameters. We also note that the use of formula (5), due to the presence of derivatives in it and their difference, requires high-quality of data on shear moduli G and μ, and a very good result of calculation of heat flux W made with such data available (see Fig. 8) quite definitely testifies to its adequacy.

Experiments and calculations similar to those presented in Fig. 8 were repeated many times for various MGs with the same result: Eqn (5) in all cases very well describes the experimental calorimetric data [28]. This implies an important (paradoxical at first glance) conclusion that the relaxation of shear elasticity uniquely determines the thermal phenomena during heating of the MG, in full accordance with IT.

A question arises: is it possible to solve the inverse problem, i.e., to calculate the kinetics of the change in the shear modulus based on the known DSC thermogram? Simple transformations of Eqn (5) yield a formula for the temperature dependence of the shear modulus of MG [59],

$$G(T) = \frac{G_{rt}}{\mu_{rt}}\,\mu(T) - \frac{\rho\beta}{\dot{T}}\int_{T_{rt}}^{T_x} W(T)\,\mathrm{d}T, \qquad (6)$$

where G_{rt} and μ_{rt} are the shear moduli of glass and crystal at room temperature T_{rt}, respectively, and T_x is the temperature of complete crystallization. An example of calculating the shear modulus based on the measured DSC thermogram using Eqn (6) is compared with the measurement in Fig. 9. As can be seen, the calculation reproduces fairly well the measured temperature dependence of the shear modulus. It should be noted again that this calculation yields the correct crystallization kinetics. Similar results were obtained for a number of other MGs [59, 60].

The change in molar enthalpy ΔH_{sr} during structural relaxation of the MG in the IT is determined by the change in the number of defects ΔN_{sr} per mol, i.e.,

$$\Delta H_{sr} = H_i \Delta N_{sr} = H_i \Delta c_{sr} N_A\,, \qquad (7)$$

where N_A is the Avogadro number, H_i is the enthalpy of formation of a single defect, according to (1) $H_i = \alpha\Omega G$, and

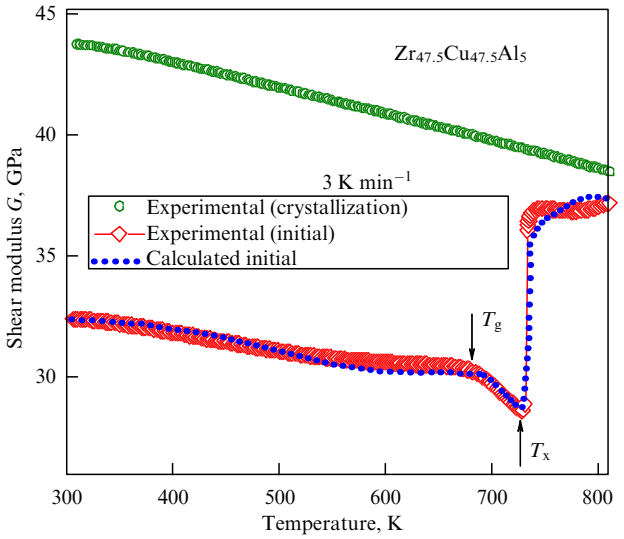

Figure 9. Experimental temperature dependence $G(T)$ of the shear modulus of $Zr_{47.5}Cu_{47.5}Al_5$ MG along with the result of its calculation based on the DSC thermogram using Eqn (6). Dependence $\mu(T)$ measured after complete crystallization is also shown [60].

the change in concentration Δc_{sr} is associated with a change in the shear modulus, which can be calculated taking into account Eqn (2) as

$$\Delta c_{sr}(T) = c(T) - c_{rt} = \frac{1}{\alpha\beta}\ln\frac{G_{rt}}{G(T)}\frac{\mu(T)}{\mu_{rt}}\,, \qquad (8)$$

where the subscript 'rt' again corresponds to room temperature, and the other quantities are defined earlier. On the other hand, the heat flux W_{gl} from the MG sample and the heat flux W_{cr} from the same sample after complete crystallization can be calorimetrically measured, which will make it possible to calculate the change in molar enthalpy as

$$\Delta H_{sr}(T) = \frac{1}{\dot{T}}\int\big(W_{gl}(T) - W_{cr}(T)\big)\,\mathrm{d}T. \qquad (9)$$

If the above reasoning is correct, then an unambiguous correlation should exist between the calorimetrically determined change in molar enthalpy according to Eqn (9) and the change in the number of defects calculated from the relaxation of the shear modulus according to Eqn (8). An example of the corresponding results for a Zr-based glass is shown in Fig. 10, from which one can see that $\Delta H_{sr}(T)$ and $H_i\Delta N_{sr}(T)$ are virtually equal at all temperatures, indicating the adequacy of relation (7), similar to other MGs [61].

We now provide another interesting example indicating a close relationship between thermal effects and shear modulus relaxation, which, according to the basic IT hypothesis (Eqn (2)), reflects a change in the concentration of defects. According to the IT, the heat Q absorbed when the MG is heated from room temperature T_{rt} to a certain temperature T_{sql} in the supercooled liquid state (i.e., in the temperature range $T_g \leqslant T_{sql} \leqslant T_{cr}$ (see Figs 7 and 8)) can be defined as [62]

$$Q = \frac{1}{\beta\rho}\left(G_{T_{rt}} - G_{T_{sql}} - \mu_{T_{rt}} + \mu_{T_{sql}}\right), \qquad (10)$$

where $G_{T_{rt}}$, $G_{T_{sql}}$, $\mu_{T_{rt}}$, and $\mu_{T_{sql}}$ are the shear moduli of glass and crystal at room temperature T_{rt} and temperature T_{sql} in

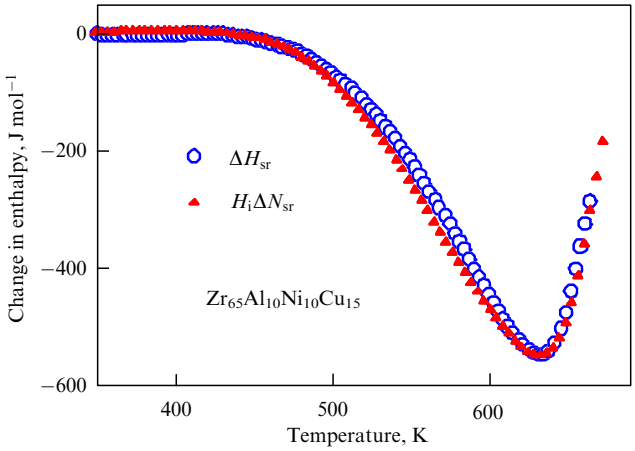

Figure 10. Change in enthalpy $\Delta H_{sr}(T)$ during structural relaxation calculated on the basis of calorimetric data using Eqn (9) for $Zr_{65}Al_{10}Ni_{10}Cu_{15}$ MG and the change in enthalpy calculated using Eqn (7), where the change in the concentration of defects is determined according to formula (8) using the data according to shear modulus relaxation for the same MG. It can be seen that $\Delta H_{sr}(T)$ and $H_i \Delta N_{sr}(T)$ are virtually equal at all temperatures, in accordance with Eqn (7) [61].

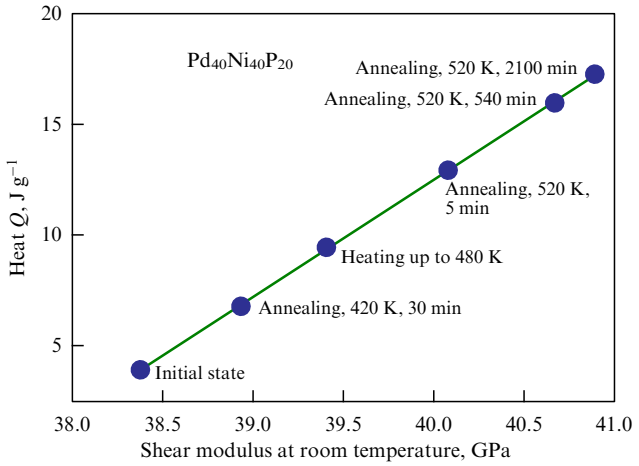

Figure 11. Integral heat Q as a result of heating $Pd_{40}Ni_{40}P_{20}$ MG to the state of a supercooled liquid as a function of the shear modulus at room temperature G_{rt} varied as a result of the heat treatments indicated in the figure. Linearity of dependence $Q(G_{sr})$ and slope $dQ/dG_{rt} = 1/(\beta\rho)$ correspond to dependence (10) [62].

the supercooled liquid state, respectively. In this case, the moduli $G_{T_{sql}}$, $\mu_{T_{rt}}$, and $\mu_{T_{sql}}$ do not depend on the thermal prehistory, but are only determined by temperatures T_{rt} and T_{sql}. Then, according to Eqn (10), heat Q should depend linearly on shear modulus $G_{T_{rt}}$ at room temperature, which in turn can be changed by preliminary heat treatment. The slope of this dependence should be $dQ/dG_{rt} = 1/(\beta\rho)$. The results of experimental verification of Eqn (10) for a Pd-based glass are presented in Fig. 11, which shows heat Q as a function of shear modulus G_{rt} at room temperature varied by the indicated heat treatment procedures. As can be seen, the $Q(G_{rt})$ dependence is indeed linear, and its slope coincides with its theoretical value quoted above with an accuracy of several percent [62]. These and similar results [63] confirm the conclusion about the relationship between thermal phenomena during heating of MG and the relaxation of their shear elasticity.

6. Volume relaxation kinetics. Dimensionless relaxation parameter

Heat treatment of MG is known to cause relaxational volume changes [64]. These changes can be interpreted in terms of the IT on the basis of the expected changes in the MG volume when defects with properties of interstitial dumbbells are introduced.

The introduction of interstitial dumbbells and vacancies into a crystal are known to cause a comparable increase ΔV in the volume, which can be represented as [19, 65]

$$\frac{\Delta V}{\Omega} = r \pm 1\,, \tag{11}$$

where Ω is the volume per atom, the minus sign corresponds to interstitial dumbbells, and the plus sign, to vacancies. Dimensionless parameter r is called the relaxation volume, which is different for vacancies and interstitial dumbbells (i.e., $r = r_v$ and $r = r_i$, respectively). Formula (11) has a simple interpretation: -1 corresponds to a change in volume when an atom moves from the surface into the crystal, and $+1$ corresponds to an increase in volume when an atom is transferred from the inner part of the crystal to its surface. The relaxation volume ($r = r_v$ or $r = r_i$) reflects the subsequent relaxation of the volume. We emphasize that the relaxation volumes for vacancies and interstitial atoms are very different, for example, for aluminum $r_i = 1.9$ [65], while $r_v = -0.38$ [19].

If a concentration of interstitial defects c is created, the relative volume change is represented as

$$\frac{\Delta V}{V} = (r_i - 1)c\,. \tag{12}$$

Equation (12) in the IT can be applied to relaxation changes in the MG volume. Then, taking into account basic hypothesis (2), it is easy to derive a change in the density during structural relaxation of the MG in the form

$$\frac{\Delta\rho}{\rho_0} \approx (r_i - 1)\Delta c = \frac{r_i - 1}{\alpha\beta} \ln\frac{G}{G_0}\,, \tag{13}$$

where density ρ_0 corresponds to the state with shear modulus G_0. With an appropriate choice of parameters, formula (13) correctly describes the increase in the MG density, depending on the increase in the shear modulus during structural relaxation of the MG [66].

Similarly, one can calculate the relative change in density during heating up to the state of complete crystallization [67]:

$$\frac{\Delta\rho(T)}{\rho_{rt}} = \frac{r_i - 1}{\beta} \ln\left(\frac{\mu_{rt}}{G_{rt}}\frac{G(T)}{\mu(T)}\right), \tag{14}$$

where subscript 'rt' corresponds to room temperature.

Results of calculations (red curves) based on Eqn (14) and experiments (blue symbols) are compared in Fig. 12. As can be seen, the calculation reproduces fairly well the relaxation (i.e., after subtracting the anharmonic component) changes in density, during both structural relaxation and crystallization, both for the initial sample (Fig. 12a) and for the sample preliminarily relaxed by heating to $T > T_g$ (Fig. 12b). We emphasize that the values of the relaxation volume r_i in studies [66, 67] were chosen to be equal to those for interstitial atoms in the corresponding crystalline metals,

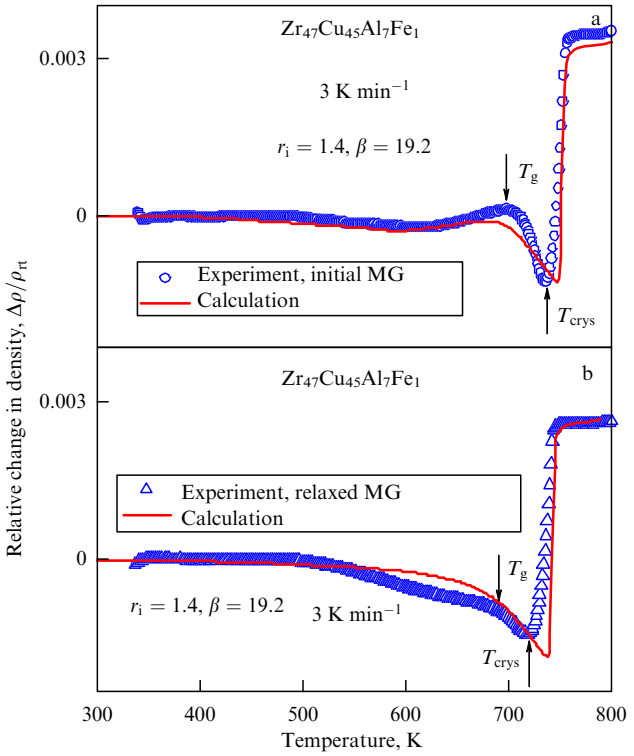

Figure 12. Relaxation changes (blue symbols) in the density of $Zr_{47}Cu_{45}Al_7Fe_1$ MG in the initial (a) and relaxed (b) states in comparison with the results of calculations by Eqn (14) (red curves) with the parameters r_i and β [67] shown in the plot.

which in a certain way indicates the nature of the considered relaxations of the MG volume.

The above difference in the values of the relaxation volume for interstitial atoms and vacancies, taking into account the fact that the latter cause a much weaker diaelastic effect (decrease in the shear modulus with the introduction of defects), makes it possible to formulate a new interesting approach to the analysis of the nature of relaxation volume changes both in crystals and in MG. In the presence of interstitial atoms and vacancies, the decrease in the shear modulus can be represented as [68]

$$\frac{\Delta G}{G} = \frac{\Delta G_i + \Delta G_v}{G} = -\beta_i c_i - \beta_v c_v \,, \qquad (15)$$

where ΔG_i and ΔG_v are the changes in the shear modulus in the presence of interstitial atoms and vacancies with concentrations c_i and c_v, respectively, and β_i and β_v are the shear susceptibilities for these defects. The influence of interstitial defects on the shear modulus is much stronger: for example, $\beta_i = 31$ for copper and $\beta_i = 27$ for aluminum, while $\beta_v \approx 2$ for vacancies [17, 37]. Taking into account Eqns (12) and (15) for interstitial atoms, we can write

$$\mathrm{d}\ln V_i = (r_i - 1)\,\mathrm{d}c_i \,, \quad \left(\frac{\mathrm{d}G}{G}\right)_i = (\mathrm{d}\ln G)_i = -\beta_i\,\mathrm{d}c_i \,. \qquad (16)$$

Similarly, for vacancies we have

$$\mathrm{d}\ln V_v = (r_v + 1)\,\mathrm{d}c_v \,, \quad \left(\frac{\mathrm{d}G}{G}\right)_v = (\mathrm{d}\ln G)_v = -\beta_v\,\mathrm{d}c_v \,. \qquad (17)$$

Eliminating $\mathrm{d}c_i$ and $\mathrm{d}c_v$ from Eqns (16) and (17), one can determine the dimensionless relaxation parameters for interstitial atoms and vacancies, respectively [68]:

$$K_i = \left(\frac{\mathrm{d}\ln G}{\mathrm{d}\ln V}\right)_i = -\frac{\beta_i}{r_i - 1} \,, \quad K_v = \left(\frac{\mathrm{d}\ln G}{\mathrm{d}\ln V}\right)_v = -\frac{\beta_v}{r_v + 1} \,. \qquad (18)$$

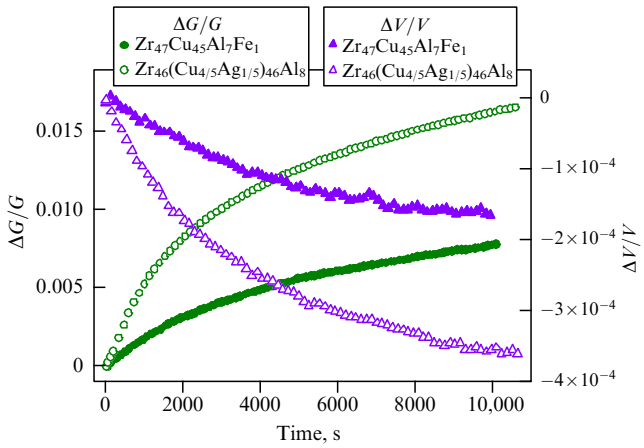

Figure 13. Kinetics of relative changes in shear modulus $\Delta G/G$ and volume $\Delta V/V$ for $Zr_{47}Cu_{45}Al_7Fe_1$ MG at $T = 523$ K and $Zr_{46}(Cu_{4/5}Ag_{1/5})_{46}Al_8$ MG at $T = 555$ K [68].

To estimate the values of K_i and K_v, we can take the above estimates of β_i, β_v, r_i, and r_v for aluminum, from which we obtain $K_i \approx -30$ and $K_v \approx -3$ for interstitial atoms and vacancies, respectively. Thus, K_i exceeds K_v by an order of magnitude, thereby reflecting a much greater influence of interstitial atoms on the shear modulus, despite the comparability of volume effects upon the insertion of interstitial atoms and vacancies. Therefore, the value of parameter K can be used to make a conclusion regarding the nature of relaxation processes, not only in crystals but also in MG, taking into account the main IT hypothesis about the role of interstitial atoms in the formation and evolution of metallic noncrystalline materials [68].

Computer modeling of Al and FeNiCrCoCu crystals has shown that the inequality $K_i \geqslant K_v$ is indeed satisfied [68]. The results of determining the parameter $K = \mathrm{d}\ln G/\mathrm{d}\ln V$ for MG can be illustrated as follows.

Figure 13 shows the kinetics of relative changes in shear modulus and volume during structural relaxation of two MGs, reflecting the standard increase in modulus and decrease in volume. The curves in Fig. 13 at the presented time scales exhibit a logarithmic time dependence [69]. At very long exposures, the nature of the kinetic dependences can change, showing the presence of two scales of temporal relaxation, which also finds an explanation in the IT [69].

Figure 14 shows the same data as the dependence of $\Delta G/G$ on $\Delta V/V$. As can be seen, the dependences almost perfectly coincide with a straight line with the parameter $K = \mathrm{d}\ln G/\mathrm{d}\ln V = -44$ [68]. Similar studies for five MGs confirmed the linearity of the dependences $\Delta G/G = f(\Delta V/V)$, and the corresponding values of the parameter K turned out to lie in a rather narrow range $(-45 \leqslant K \leqslant -38)$ [68]. Note that the relaxation of the shear modulus and volume of single-crystal Al due to a change in the concentration of interstitial atoms corresponds to $K = -36$ [68]. The following conclusion can be drawn: the experimentally observed values of $K \approx -42$ confirm the IT hypothesis that

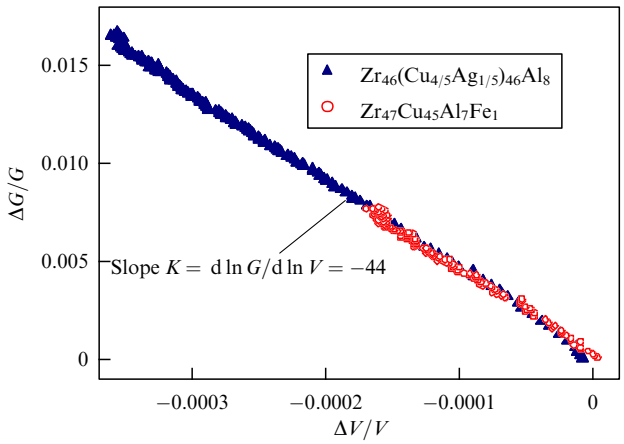

Figure 14. Rearrangement of relaxations of the shear modulus and volume shown in Fig. 13 in coordinates $\Delta G/G = f(\Delta V/V)$. Angular coefficient corresponds to parameter $K = \mathrm{d}\ln G/\mathrm{d}\ln V = -44$ [68].

the relaxation phenomena in MGs are due to the evolution of defects such as dumbbell interstitials.

7. Fragility and heat capacity jump

It is generally accepted that the most important kinetic parameter of supercooled liquids and glasses is shear viscosity η. Of particular interest is the temperature dependence of η in the vicinity of glass transition temperature T_g. As noted by S V Nemilov [70], this interest arose from the production experience of the early 1920s, namely, the accepted division of glasses into 'short' and 'long.' These terms are related to the length of the interval between the lower temperature of the processing of the supercooled melt and the temperature at which a sharp decrease in its viscosity begins. The width of this interval, which reflects the rate of change in viscosity with temperature in the supercooled liquid state, is an important technological parameter. In the 1980s–1990s, this property was characterized by the introduction of a dimensionless fragility index (more often called fragility), defined as [71–73]

$$m_\eta = \left.\frac{\mathrm{d}\log\eta}{\mathrm{d}(T_g/T)}\right|_{T=T_g}, \tag{19}$$

where T_g is the temperature at which the viscosity η of the supercooled liquid is 10^{12} Pa s. This definition of glass transition temperature T_g is considered to be its standard definition, and fragility m_η characterizes the rapidity of melt freezing upon cooling to a temperature close to T_g. Supercooled melts with a higher m_η (i.e., 'short' melts) feature a relatively narrow supercooled liquid temperature range, while low m_η melts ('long' melts) exhibit a relatively wide interval, in which supercooled liquid exists. It is also important that fragility determines the degree of deviation of the temperature dependence of viscosity from the Arrhenius one. In the case of purely Arrhenius behavior, $m_\eta \approx 16$, the supercooled liquid is considered 'strong,' and its structure does not change with temperature. Usually, MGs with a fragility of less than 50 are considered strong. An increase in m_η corresponds to an increasingly large change in structure with temperature, and glasses with m_η above 50–60 are considered 'fragile.'

It is of importance to emphasize that fragility correlates with various properties of MGs: critical cooling rate, glass-forming ability, excess entropy, Poisson's ratio, shear modulus, low-temperature vibrational properties, yield strength, hardness, etc. [74]. The nature of such correlations remains unclear. On the whole, it can be asserted that fragility m_η is an important physical parameter associated with the properties of supercooled liquids and glasses. However, the specific mechanisms of this connection remain unclear.

Fragility m_η can be calculated in the IT. To do so, the widely used assumption of 'elastic models' of glass transition can be accepted, according to which the activation of elementary rearrangements is controlled by the elastic resistance of the medium, which is determined by instantaneous shear modulus G [75]. Moreover, the shear viscosity can be represented as [76, 77]

$$\eta(T) = \eta_0 \exp\left(\frac{G_{sql}(T)V_c}{k_B T}\right), \tag{20}$$

where G_{sql} is the shear modulus in the supercooled liquid state, V_c is the characteristic volume of the elementary rearrangement, and pre-exponential $\eta_0 = N_A h/V_\mu \sim 10^{-4}$ Pa s (h is Planck's constant and V_μ is the molar volume) [78].[3] Using further the main equation of the IT (2), one can calculate the fragility as [74]

$$m_G = \left(1 - T_g\frac{\mathrm{d}\ln G_{sql}}{\mathrm{d}T}\right)\log_{10}\frac{\eta_g}{\eta_0}, \tag{21}$$

where T_g is the glass transition temperature for the chosen heating rate, and $\eta_g = 10^{12}$ Pa s. Equation (21) makes it possible to determine the fragility if the temperature dependence of the shear modulus G_{sql} in the supercooled liquid state is known.

To assess the adequacy of Eqn (21), dedicated experiments were carried out to measure the high-frequency shear modulus and shear viscosity of seven MGs [74]. Based on measurements of the shear modulus, fragility m_G was calculated using Eqn (21), and the measurements of shear viscosity were used to calculate fragility m_η based on Eqn (19). It is shown that $m_G \approx m_\eta$ with an accuracy of no worse than 9–10%, thereby confirming the correctness of the IT calculation of m_G. Thus, it can be argued that the fragility of MG is determined by the rate of change in the shear modulus in the state of a supercooled liquid. Moreover, the temperature derivative of the defect concentration $\mathrm{d}c/\mathrm{d}T$ is constant in this state and, correspondingly, the concentration of defects increases at a constant rate. Consequently, as it turns out, the fragility becomes greater as the defect generation rate rises.

On the other hand, it is well known that fragility m_η is associated with a jump in heat capacity ΔC_{sql} upon transition through the state of a supercooled liquid, and the larger $m_\eta \approx m_G = m$, the stronger this jump is [70, 80]. The specific mechanism of this relation is not discussed in the literature. However, an IT-based analysis gives an expression for the heat capacity jump in the form [74]

$$\Delta C_{sql} = \frac{G_{sql}}{\rho\beta T_g}\left(\frac{m}{\log(\eta_g/\eta_0)} - 1\right), \tag{22}$$

i.e., the jump in heat capacity ΔC_{sql} actually increases with increasing fragility m. In addition, the value of ΔC_{sql} is

[3] The connection between quantity η_0 and Planck's constant was discussed in detail in recent paper [79].

proportional to the shear modulus G_{sql} of the supercooled liquid and inversely proportional to density ρ, shear susceptibility β, and glass transition temperature T_g. For metallic glasses, the estimates of ΔC_{sql} based on Eqn (22) agree with the experimental data [74].

8. Excess thermodynamic potentials

One of the ways to study MGs is related to the determination of MGs' thermodynamic potentials and calculation of the properties on this basis. This approach, first implemented in the 1990s [81, 82], is still used today [83, 84]. The general scheme of these studies is to employ data on heat capacity at temperatures above and below T_g in combination with data on the heat and/or entropy of melting to calculate excess enthalpy ΔH, entropy ΔS, and the Gibbs potential $\Delta\Phi$ of a supercooled liquid and/or glassy states with respect to the corresponding values of the crystalline state. The results obtained are primarily used to estimate the glass-forming ability of supercooled melts and the kinetics of their crystallization. The physical nature of excess thermodynamic potentials remains largely outside the field of vision.

However, the excess thermodynamic potentials of MGs with respect to the thermodynamic potential of the parent crystal can be determined on the basis of calorimetric data, for which DSC data on the heat flux for the initial glass sample W_{gl} and the same sample after complete crystallization W_{cr} are required. Then, the temperature dependence of the excess enthalpy can be calculated from the formula [85, 86]

$$\Delta H_Q(T) = \frac{1}{\dot{T}} \int_T^{T_x} \Delta W(T)\, \mathrm{d}T, \tag{23}$$

where $\Delta W = W_{gl} - W_{cr}$ is the difference heat flux and T_x is the temperature of complete crystallization. The excess entropy can then be defined as

$$\Delta S_Q(T) = \frac{1}{\dot{T}} \int_T^{T_x} \frac{\Delta W(T)}{T}\, \mathrm{d}T, \tag{24}$$

and the Gibbs potential is calculated using the standard formula $\Delta\Phi_Q = \Delta H_Q - T\Delta S_Q$. The subscript Q emphasizes that the values are determined from calorimetry data. Note that excess entropy ΔS_Q here includes vibrational and concentration components. We also emphasize that, according to definitions (23) and (24), the quantities ΔH_Q and ΔS_Q vanish when the value of T reaches the temperature of complete crystallization T_x. In other words, quantities ΔH_Q, ΔS_Q, and $\Delta\Phi_Q$ only reflect the contribution of the structural state of the MG (i.e., their noncrystallinity per se) to the thermodynamic potentials and, in this sense, are indeed excessive with respect to the parent crystalline state. By the way, despite the obvious simplicity of definitions (23) and (24), the corresponding calculations were first performed quite recently [85, 86].

Figure 15 shows as an example calculation of ΔH_Q, ΔS_Q, and $\Delta\Phi_Q$ for the $Cu_{49}Hf_{42}Al_9$ MG. As can be seen, ΔH_Q and ΔS_Q remain almost constant at $T < T_g$, increase by about a quarter at T between T_g and the crystallization onset temperature, and then rapidly decrease to zero as a result of complete crystallization at T_x. At the same time, the excess Gibbs potential $\Delta\Phi_Q$ decreases almost linearly to zero at $T \approx T_x$. Similar results were also obtained for other MGs [85].

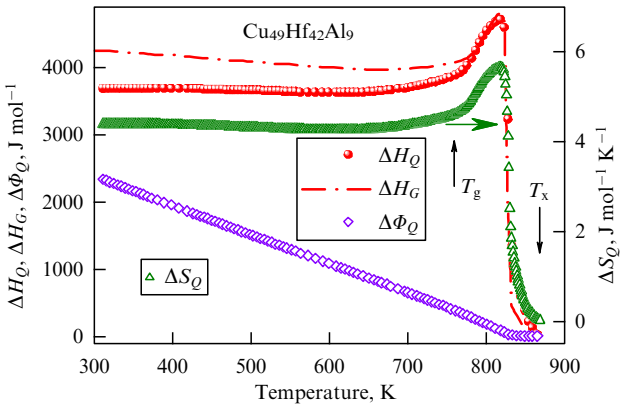

Figure 15. Temperature dependences of excess enthalpy ΔH_Q and excess entropy ΔS_Q (calculated using Eqns (23) and (24), respectively, based on calorimetric measurements) and excess Gibbs potential $\Delta\Phi_Q$ for the $Cu_{49}Hf_{42}Al_9$ MG. Temperature dependence ΔH_G was determined from Eqn (25) using data on shear modulus relaxation [85].

On the other hand, the excess enthalpy can be independently determined in the IT based on the measurements of the shear modulus [28, 87] as

$$\Delta H_G(T) = \frac{N_A \Omega}{\beta}\big(\mu(T) - G(T)\big)\,. \tag{25}$$

The results of the calculation of ΔH_G by Eqn (25) using the experimentally determined dependences $G(T)$ and $\mu(T)$ for the $Cu_{49}Hf_{42}Al_9$ MG are also shown in Fig. 15. As can be seen, ΔH_G is very close to the calorimetrically determined ΔH_Q at $T < T_g$ and virtually coincides with it at higher temperatures. A similar situation occurs for other MGs: the deviation of ΔH_G from ΔH_Q does not exceed 10–15% [85, 86].

However, the main implication of Eqn (25) is that it determines the elastic energy of the system of interstitial-type defects frozen in from the melt as a result of its quenching [28, 86, 87]. Thus, we come to an important conclusion: all excess thermodynamic potentials of the MG with respect to the parent crystalline state (including excess internal energy ΔU_Q, which actually coincides with ΔH_Q) are almost completely determined by the elastic energy of the defect subsystem ΔU_{el}; therefore, in particular, $\Delta U_{el} = \Delta H_G \approx \Delta H_Q = \Delta U_Q$. In the process of heating, the elastic energy dissipates into heat, which determines the above-described relationship between the thermal effects and the relaxation of the shear elasticity of the MG. Notably, the crystallization heat (i.e., the exothermic effect of the transformation of a supercooled liquid into a crystal) is mainly the result of the dissipation of the elastic energy of the defect subsystem at $T > T_g$, which was confirmed by dedicated experiments [28, 86, 87]. We also note that, as an analysis of data on excess enthalpy and excess entropy showed, the enthalpy H_i of the formation of a single defect is determined by the shear modulus, while the entropy of formation S_i is very large $(10-30\,k_B)$, in accordance with the basic IT hypotheses [85, 86].

It is of interest to find out how elastic energy ΔU_{el} and excess entropy ΔS_Q of the defect subsystem change depending on excess internal energy ΔU_Q when the chemical composition of the MG is varied. The corresponding results for ten MGs are shown in Fig. 16 [86]. It can be seen, first, that $\Delta U_{el} \approx \Delta U_Q$ (the slope for this dependence is equal to unity),

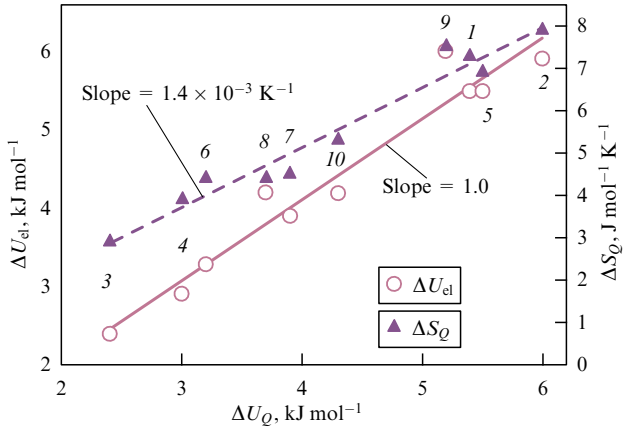

Figure 16. Elastic energy $\Delta U_{el} = \Delta H_G$ of the subsystem of the system of defects calculated by Eqn (25) using data on the shear modulus and excess entropy ΔS_Q determined by relation (30) using DSC data as functions of the excess internal energy $\Delta U_Q = \Delta H_Q$ calculated by Eqn (23) on the basis of calorimetric data for various MGs: *1* — $Zr_{47.5}Cu_{47.5}Al_5$, *2* — $Zr_{48}Cu_{48}Al_4$, *3* — $Zr_{50}Cu_{40}Al_{10}$, *4* — $Zr_{47}Cu_{45}Al_7Fe_1$, *5* — $Zr_{46}(Cu_{4/5}Ag_{1/5})_{46}Al_8$, *6* — $Zr_{52.5}Ti_5Cu_{17.9}Ni_{14.6}Al_{10}$, *7* — $Zr_{55}Co_{25}Al_{20}$, *8* — $Cu_{49}Hf_{42}Al_9$, *9* — $Pd_{40}Ni_{40}P_{20}$, *10* — $Ti_{16.7}Zr_{16.7}Hf_{16.7}Cu_{16.7}Ni_{16.7}Be_{16.7}$ [86].

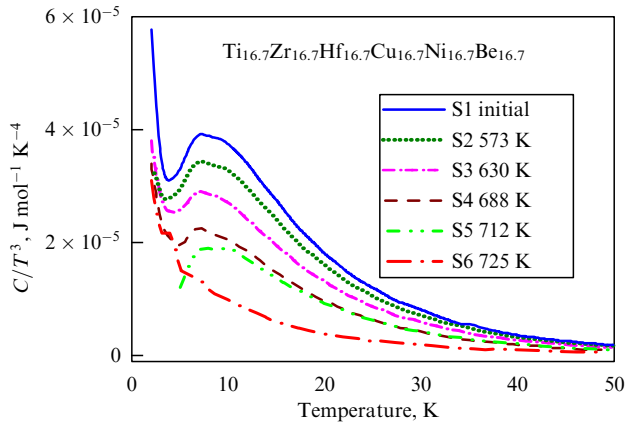

Figure 17. Bosonic peak in heat capacity in $Ti_{16.7}Zr_{16.7}Hf_{16.7}Cu_{16.7}Ni_{16.7}Be_{16.7}$ metallic glasses for original and annealed samples after subtracting components due to free electrons and two-level systems [93].

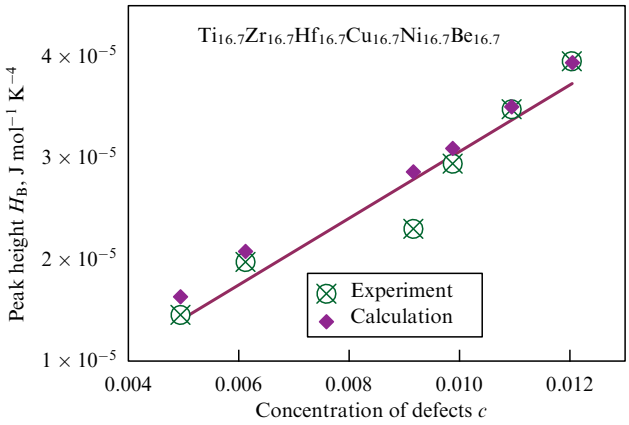

Figure 18. Comparison of experimental and calculated (using Eqn (26)) heights of the boson peak of heat capacity in $Ti_{16.7}Zr_{16.7}Hf_{16.7}Cu_{16.7}Ni_{16.7}Be_{16.7}$ metallic glasses as a function of the concentration of defects determined from measurements of the shear modulus [93].

as noted above (see Fig. 15). Second, excess entropy ΔS_Q increases linearly with the increase in excess internal energy ΔU_Q. Finally, even small variations in the chemical composition of MGs can result in very significant changes in both the elastic energy of defects and the excess internal energy and entropy (see, for example, compositions *1* and *3*). It can be assumed that MGs with maximum values of ΔU_{el} and ΔS_Q (in particular, compositions *1*, *2*, *5*, and *9* in Fig. 16) exhibit the maximum tendency to relaxation of physical properties, which can manifest itself, for example, in the magnitude of thermal effects, relaxation of the shear modulus, and changes in shear viscosity during heating. In this connection, it can be noted that the difference $\mu - G \approx \mu\alpha\beta c$ entering Eqn (25) is proportional to the concentration of defects. Therefore, as can be expected, MGs with the maximum concentration of frozen-in defects will show the maximum tendency to relaxation.

9. Boson peak of heat capacity

The boson peak of heat capacity is a low-temperature (5–15 K) heat capacity anomaly C_p, which manifests itself as a peak in the temperature dependence of the C_p/T^3 value. It is generally accepted that this anomaly is associated with an excess (above Debye) vibrational density of states, which is observed in the terahertz range in measuring neutron and Raman scattering. Such universal features are observed for all noncrystalline materials [88, 89], including MGs [90]. The physical mechanism of the boson peak of heat capacity, despite many years of research and numerous interpretations of its physical nature, remains largely unclear [53, 91, 92].

Figure 17 shows, as a typical example, the boson peak of heat capacity in the MG in the initial state and after the specified heat treatments [93]. As always, as a result of annealing, the peak height decreases, and the shear modulus increases significantly [92–94].

However, the boson peak can be naturally interpreted in terms of the IT. Granato suggested that interstitial defects behave like Einstein oscillators, and their low-frequency vibrational modes (mentioned in Sections 2 and 4) contribute to the heat capacity [95], boson peak height H_B being proportional to defect concentration c. After some refinements, the expression for H_B takes the form [92, 96]

$$H_B = \frac{C_i}{T_B^3} = \frac{234\,R}{\Theta_D^3}\left[0.09 f \left(\frac{\omega_D}{\omega_r}\right)^3 + \frac{3}{2}\beta\right] c = \Gamma c\,, \qquad (26)$$

where T_B is the peak temperature, C_i is the heat capacity associated with interstitial defects, Θ_D and ω_D are the Debye temperature and frequency, respectively, ω_r is the characteristic frequency of resonant oscillations of defects, f is the number of resonant modes per defect, R is the universal gas constant, and defect concentration c can be estimated from measurements of the shear modulus using Eqn (2). Figure 18 compares the value of H_B determined using formula (26) with its experimental value. The calculation was carried out with the characteristic number of modes for an interstitial dumbbell $f = 5$ and the ratio $\omega_D/\omega_r = 5$ (which, according to Granato's estimate, is equal to seven [95]). As can be seen, the calculation results are in good agreement with the experimental data, and H_B actually increases linearly with

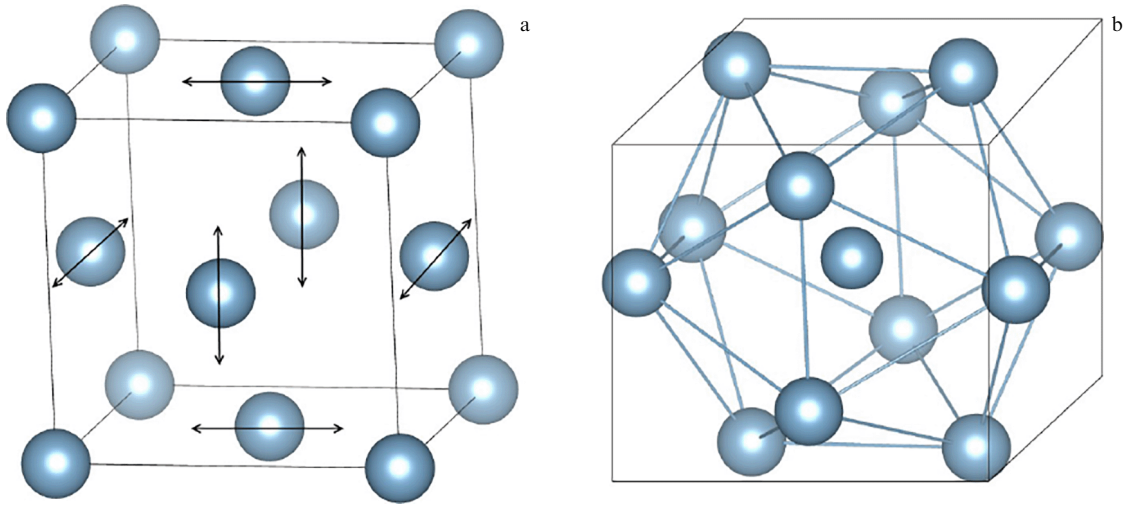

Figure 19. Formation of an ideal icosahedron by creating interstitial dumbbells on opposite faces of an fcc cell. (a) Elementary fcc cell; arrows show how two atoms should be placed instead of one. (b) Ideal icosahedron with Voronoi indices $\langle 0, 0, 12, 0\rangle$ formed by six interstitial dumbbells on the cell faces and one interstitial atom in an octahedral position, i.e., in the center of the cell [28, 97].

an increase in the defect concentration, both in the completely amorphous [93] and in the partially crystallized state [96].

On the other hand, calorimetric measurements make it possible to calculate the change in enthalpy during heat treatment as $\Delta H = \dot{T}^{-1} \int \Delta W \, \mathrm{d}T$, where ΔW is the differential heat flux (see Eqn (23)), and the integral is calculated in a temperature range from the onset of structural relaxation to complete crystallization of the MG. The same enthalpy change can be determined from formula (25) by assuming that the shear moduli of glass G and crystal μ are equal to their values at room temperature. Then, expressing the concentration of defects from Eqn (2) and expanding it into a series, it is easy to obtain the relation $\Delta H = \mu N_{\mathrm{A}} \Omega / c$. Hence, taking into account formula (26), we find for the height of the boson peak

$$H_{\mathrm{B}} = \Gamma c = \frac{\Gamma}{\mu N_{\mathrm{A}} \Omega} \Delta H \,, \tag{27}$$

where the quantity Γ is determined by Eqn (26). It can be seen that the height of the boson peak should be proportional to the value of ΔH, which, in essence, is the excess enthalpy of the MC. It is this dependence that is observed experimentally [93].

Thus, the IT provides an adequate description of the boson peak of the heat capacity based on the concept of low-frequency resonant vibrational modes of defects such as dumbbell interstitials. In this connection, a recent molecular dynamics study should be noted [53], whose authors showed that the boson peak of heat capacity emerges when interstitial dumbbells are introduced into a CuNiCoFe crystal, and its height is proportional to their concentration. Moreover, the boson peak in a crystal is quite similar to that observed in glass of the same composition.

10. Clustering of defects as a probable mechanism for the evolution of a defect subsystem

IT-based estimates show that the concentration of interstitial defects in MG is at least 2–3%. It is clear that, at such a high concentration, interstitial defects should effectively interact with each other. In Granato's original theory [14, 15], an interstitial defect was modeled in the form of a string, and the interaction among defects was qualitatively described in terms of 'crossings' of strings with each other, and the final result was expressed as a phenomenological dependence of the parameters of 'strings' on their concentration. However, the representation of a dumbbell interstitial as an elastic dipole (see Sections 2 and 4) makes it possible to construct a more specific mechanism for changing the properties of a system of interstitial defects with a change in concentration. Back in the 1980s, it was established that dumbbell (split) interstitials (elastic dipoles) can form clusters consisting of two or more (up to 7–10) individual interstitials [97]. A cluster of seven interstitial atoms in an fcc structure forms a regular icosahedron, as shown in Fig. 19. Such clustering is energetically favorable, in connection with which a possible connection between the features of the structural relaxation of the MG and the clustering processes of elastic dipoles was hypothesized [69]. The emergence of such a hypothesis was preceded by numerous studies indicating the presence and important role of icosahedral ordering in metallic glasses [5, 98–100].

The clustering of elastic dipoles was examined in detail by means of molecular dynamics simulation using the example of aluminum as a convenient model subject [101]. Primarily, the specific (per interstitial atom) characteristics of dipoles in single-crystal Al during their clustering were studied. As expected, the specific formation enthalpy (normalized to the number of interstitials in a cluster) decreases fairly rapidly with decreasing cluster size, but for large clusters (containing six or more interstitials) it reaches an approximately constant value close to 1/2 of the enthalpy of formation of a single dumbbell. The vibrational density of states sharply changes its character starting from clusters of four interstitials, as shown in Fig. 20. As can be seen, while a single dumbbell and clusters consisting of two and three dipoles exhibit a clearly pronounced low-frequency anomaly in the spectrum, for large clusters it virtually disappears. This phenomenon is also manifested in the vibrational spectrum. Indeed, Fig. 21 shows that the atoms of an ideal icosahedron do not contribute to the low-frequency part of the spectrum, while

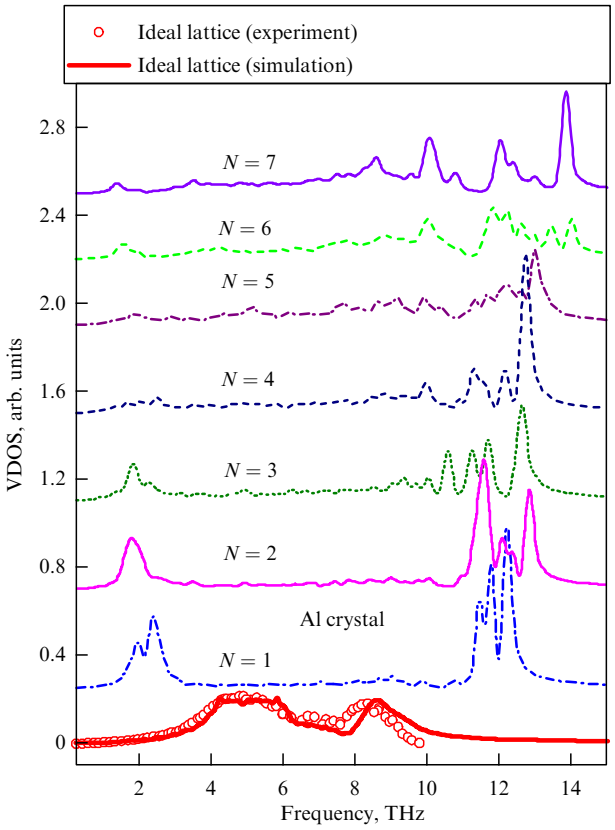

Figure 20. Vibrational density of states for an ideal lattice (simulation and experiment results); its change with an increase in the number of interstitial atoms in a cluster from a single interstitial dumbbell ($N = 1$) to an ideal icosahedron containing $N = 7$ interstitial atoms [101].

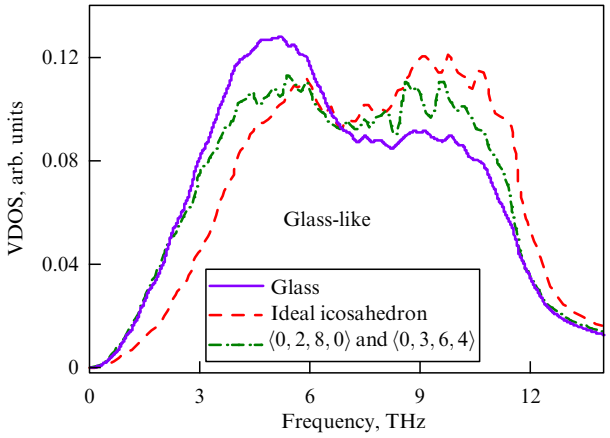

Figure 21. Vibrational spectra for all atoms of the glass-like aluminum model, atoms of an ideal icosahedron ($N = 7$, Voronoi indices $\langle 0, 0, 12, 0\rangle$), and atoms with Voronoi indices $\langle 0, 2, 8, 0\rangle$ and $\langle 0, 3, 6, 4\rangle$ corresponding to a single interstitial dumbbell ($N = 1$) in the crystal [101].

the averaged spectrum of the entire model glass, including its low-frequency part, is quite close to the spectrum of interstitial atoms in a crystal corresponding to the Voronoi indices $\langle 0, 2, 8, 0\rangle$ and $\langle 0, 3, 6, 4\rangle$.

No less interesting is the behavior of the local vibrational entropy per atom for crystalline and glass-like Al depending on the number of interstitials in the cluster (Fig. 22). It can be seen that, with an increase in the number of atoms in a cluster, the vibrational entropy sharply decreases: for $N > 4$, it is

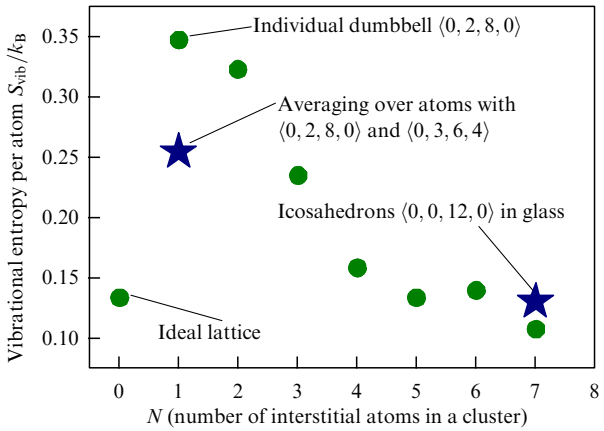

Figure 22. Vibrational entropy per atom S_{vib} for crystalline (green dots) and glass-like Al (blue stars) versus the number of interstitial atoms N in a cluster. S_{vib} decreases with increasing N in the crystal, so the entropy for an ideal icosahedron ($N = 7$) is even slightly less than for an ideal lattice. Star on the left side of the plot corresponds to the entropy of the Al glass averaged over atoms with Voronoi indices $\langle 0, 2, 8, 0\rangle$ and $\langle 0, 3, 6, 4\rangle$ ($N = 1$, separated dumbbells in a crystal). Star on the right side of the plot shows S_{vib} for icosahedral clusters in glass with indices $\langle 0, 0, 12, 0\rangle$ [101].

actually close to the vibrational entropy of an ideal lattice. This observation implies that clustering of dipoles cannot continue indefinitely, since the Gibbs formation potential ceases to decrease with an increase in the number of interstitials in a cluster from a certain moment, while, at a high temperature, it even begins to increase. This in turn indicates that each specific temperature corresponds to its own equilibrium ratio among the sizes of clusters in the system. In addition, as Fig. 22 shows, the clusters can be conditionally divided into two groups, with $N < 4$ and $N > 4$. Small clusters and single dipoles can be considered 'defects' that actively interact with an external stress and can quickly change their state, grouping into larger clusters or breaking up into separate dipoles. Large clusters turn out to be more stable, since, with a change in the number of atoms they contain, the specific enthalpy and entropy change much more weakly, and they can be conditionally attributed to an amorphous 'matrix' with a dominant icosahedral ordering, which, as noted above, is characteristic of MGs.

From this perspective, the evolution of the glass structure and its defect subsystem with temperature can be qualitatively represented as follows. Crystal melting occurs due to the rapid avalanche-like generation of split interstitials. With an increase in their concentration, the process of clustering begins, leading to a gradual increase in the size of clusters. However, upon reaching a certain concentration of interstitials, the process of their clustering slows down, and an ensemble is formed in the material, consisting of individual interstitials and clusters of various sizes. The ratio between their relative concentrations depends on temperature (the higher the temperature, the greater the relative concentration of small clusters). It should be noted that the equilibrium between the concentration of clusters of different sizes and individual interstitials is dynamic, i.e., clusters grow and decay concurrently. Rapid quenching of the glass 'freezes' the ratios between the concentrations of clusters of different sizes, which are characteristic of the melt. When such glass is heated, at the moment when a certain temperature is reached, the clusterization of the 'excess' part of individual dipoles and

their small clusters begins, so that, at temperatures exceeding T_g, the distribution between clusters becomes close to equilibrium for these temperatures. If the temperature increases further, the size distribution of clusters again becomes nonequilibrium, and the process of 'evaporation' (thermal decomposition) of clusters into smaller formations begins. Upon reaching temperatures close to the temperature at which crystallization begins, the size distribution between clusters becomes similar to that in the melt. Upon quenching, an unrelaxed (or weakly relaxed) glass is again formed from this state, and, upon slow cooling, repeated clustering occurs, and a relaxed state is formed. The degree of relaxation strongly depends on the cooling rate, since the clustering process is thermally activated, and already at temperatures far enough from room temperature it stops completely at the cooling rates realized in the experiment.

The presented scenario of glass evolution qualitatively describes the important features of the behavior of its properties during heat treatment. In particular, this refers to mechanisms for the nonmonotonic behavior of the shear modulus in the initial state of the glass upon heating, the increase in the shear modulus compared to that of the initial state upon slow cooling of the preheated glass, the effect of restoring the elastic characteristics to the values close to those characteristic of the initial state during quenching of glass from temperatures higher than the glass transition temperature, and the features and nature of the thermal effects that appear in this case.

11. Relation between the properties of glass and the parent crystal

As noted in the Introduction, it seems quite apparent that the properties of MG should be related to the characteristics of the parent crystal, i.e., the crystalline state that arises as a result of glass crystallization and, at the same time, is the starting material for the melt from which glass is made. Therefore, their physical characteristics must correlate with each other. However, in most models and theories of the amorphous state, this issue is not considered at all and is not even raised. The IT is the only theory in which this correlation is not only analyzed but also 'genetically' embedded in the initial hypotheses, an assertion directly following from Eqn (2), which is one of the main components of the mathematical formalism of the IT and directly shows that the shear modulus of glass G is proportional to that of the parent crystal μ. As has been repeatedly noted in this review, the shear modulus is the most important characteristic that determines the properties of the MG. First of all, it should be noted that relationship $G(\mu)$, which directly determines the thermal effects during heating of the MG, follows directly from Eqns (5), (6), and (10). This relationship sets the dependence of the MG density on temperature, which is determined by formula (14). Finally, this relationship manifests itself in the most important way in the enthalpy of the defect subsystem (25), which, as noted, is virtually equal to the elastic energy of the defect subsystem and, in essence, determines all excess thermodynamic potentials of the MG. Consequently, the parent crystal in the energy sense is the ground state of the glass, i.e., its state with the minimum energy [102].

On the other hand, the relationship between shear moduli of glass and the parent crystal is reflected in the concentration of defects, a decrease in which during relaxation or crystallization causes partial or complete release of the elastic energy of defects in the form of heat. When the defect concentration does not change (i.e., at temperatures at which there is no relaxation whatsoever), Eqn (2) can be represented as $\mathrm{d}\ln G/\mathrm{d}T = \mathrm{d}\ln\mu/\mathrm{d}T$, or

$$\frac{\mathrm{d}\ln G}{\mathrm{d}\ln\mu} = 1\,. \tag{28}$$

Formula (28) implies that, in the temperature range where there is no structural relaxation, the temperature derivatives of the relative changes in the shear modulus of glass and the shear modulus of the parent crystal should be the same. Measurements of the moduli G and μ for MGs of 24 chemical compositions have shown that relation (28) is indeed satisfied with an accuracy of about 10% or even better [103]. This, on the one hand, is an experimental confirmation of the relationship between the properties of glass and the parent crystal, and, on the other hand, is another confirmation of the adequacy of the IT.

In the Introduction, we gave a definition of the parent crystal, which is quite suitable when glass crystallization occurs in one stage, even if a multiphase polycrystalline structure is formed. However, the crystallization process often occurs in several stages, sometimes with very different temperatures, and the resulting phases can be metastable. The IT in its original version does not involve consideration of phase transformations in the crystallized state. Therefore, the concept of the parent crystal becomes not quite unambiguous. In this case, the simplest solution seems to take as such the high-temperature state from which the melt is obtained. However, in Eqns (1) and (2), it is necessary then to add elastic and thermal effects that occur in a crystallized state, which complicates the description. It should be emphasized that in most cases the main elastic and thermal effects occur at the very first stage of crystallization, and then the definition of the maternal state given in the Introduction is quite adequate.

On the other hand, the relationship among the properties of glass, melt, and parent crystal manifests itself in a very interesting way in the ratio among the enthalpies of structural relaxation, crystallization, and melting. As noted, the IT assumes the inheritance of defects such as interstitial dumbbells from the melt. If the rate of melt quenching is sufficiently large, one can expect that the concentrations of defects in the glass and melt will be approximately the same, $c_{\mathrm{glass}} \approx c_{\mathrm{melt}}$. The value of c_{glass} in the IT determines the total heat content (enthalpy) of glass. Structural relaxation of the glass at $T < T_g$ leads to a decrease in c_{glass} by a certain amount Δc_{rel}, thereby causing an increase in the shear modulus from G to $G_{\mathrm{rel}} = G\exp(\alpha\beta\Delta c_{\mathrm{rel}})$ and a corresponding decrease in the enthalpy by ΔH_{rel}. The residual concentration of defects $c_{\mathrm{melt}} - \Delta c_{\mathrm{rel}} \approx c_{\mathrm{cryst}}$ decreases to zero as a result of crystallization, and the shear modulus increases to its value μ in the crystalline state with concurrent release of enthalpy $\Delta H_{\mathrm{cryst}}$. The total heat release of the initial glass as a result of crystallization is then described by Eqn (25), where $\Delta H_G \approx \Delta H_{\mathrm{cryst}}$. Since the concentration of defects frozen in from the melt is $c_{\mathrm{melt}} \approx \Delta c_{\mathrm{rel}} + c_{\mathrm{cryst}}$, the total heat absorbed during melting should approximately equal the total heat released during structural relaxation and crystallization, i.e., in terms of the corresponding enthalpy changes, the relation

$$\Delta H_{\mathrm{melt}} \approx -(\Delta H_{\mathrm{cryst}} + \Delta H_{\mathrm{rel}}) \tag{29}$$

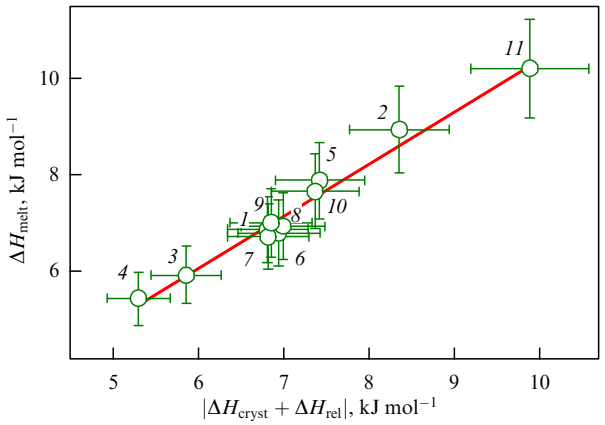

Figure 23. Melting enthalpy as a function of the absolute value of the sum of enthalpies of structural relaxation and crystallization. Numbers correspond to different MCs based on Zr, Pd, and La [28, 104]. Slope of the dependence is close to unity, which confirms the validity of Eqn (29).

should hold. The result of an experiment carried out to test relation (29) is presented in Fig. 23, which shows the enthalpy of melting of the parent melt ΔH_{melt} as a function of the absolute value of the sum of the enthalpy of structural relaxation ΔH_{rel} and the enthalpy of crystallization ΔH_{cryst} for 11 MGs based on Zr, Pd, and La [28, 104]. As can be seen, this dependence fits well into a straight line, the slope of which is close to unity, so that Eqn (29) is fulfilled with an accuracy of no worse than 10%. This fact directly confirms the IT concept that the number of defects formed during the melting of the parent crystal is approximately equal to the number of defects disappearing during the structural relaxation and crystallization of the MG, and thus the properties of the parent crystal and glass are indeed interrelated.

12. Alternative thermodynamic approach

Studies have shown that an alternative approach to describing the relationship between thermal phenomena and relaxation of shear elasticity during the structural relaxation of MG is possible, which is actually not related to the IT but leads to practically the same result.

We now consider glass as a thermodynamic system consisting of a certain matrix and a defect subsystem. Heat treatment causes the evolution of a defect subsystem, which can be interpreted as a change in the concentration of certain defects. Relaxation of the defect subsystem causes a change in the macroscopic entropy of glass by some value ΔS_d. This change in entropy can be calculated using the general thermodynamic relation [105]

$$\Delta S_d = -\frac{R_{min}}{T}\,, \tag{30}$$

where R_{min} is the minimum work that must be done to transfer the defect subsystem to a state of metastable equilibrium with the matrix, and T is the absolute temperature. Formula (30) determines to what extent the entropy of a nonequilibrium glass differs from its maximum value at a given temperature [106]. The minimum work R_{min} in Eqn (30) is determined by the Gibbs potential barrier $\Delta\Phi_d$ for elementary atomic rearrangements leading either to annihilation of defects or to their transition to other energy states. In the 'elastic models' of glass transition mentioned in Section 3, the energy barrier of elementary rearrangements is controlled by the instantaneous shear modulus G [75] and, following Eqn (20), this barrier can be represented as $\Delta\Phi_d = GV_c$, where V_c is some characteristic volume of the rearrangement.

Let the total concentration of defects c_0 include a certain concentration of defects c_{tr} that can change the structural (energy) state during heat treatment. Then, a change in the structural state of defects requires work $dR = N_A V_0 G\, dc_{tr}$ to be done and causes a change in the shear modulus [106]:

$$\frac{dG_{rel}}{G} = B\, dc_{tr}\,, \tag{31}$$

where B is the shear susceptibility characterizing the decrease in the shear modulus in the presence of defects (diaelastic effect). In the thermodynamic approach considered in this section, Eqn (31) is the only assumption about the properties of defects responsible for the structural relaxation of the MG. Combining Eqn (31) and the above formula for work, it is easy to calculate the work to be done for the relaxation change in the shear modulus given by Eqn (31):

$$dR = \frac{N_A V_0}{B}\, dG_{rel}\,. \tag{32}$$

Assuming that dR in Eqn (32) is the differential of the minimum work R_{min} in formula (30), it is possible to calculate the thermal effect with an infinitely small change in the concentration of defects and the corresponding change in the relaxation component of the shear modulus as $\delta Q = T\, dS_d = -(N_A V_0/B)\, dG_{rel}$. Then, the heat flux takes the form [106]

$$W = \frac{1}{m_\mu}\frac{\delta Q}{dt} = \frac{\dot T}{m_\mu}\frac{\delta Q}{dT} = -\frac{N_A V_0 \dot T}{m_\mu B}\frac{d(\Delta G_{rel})}{dT}\,, \tag{33}$$

where m_μ is the molar mass. The result of calculating W using Eqn (33) can be compared with the experimental results if the relaxation component of the shear modulus ΔG_{rel} is known.

To determine ΔG_{rel}, a special procedure was developed [106], which was used to calculate the heat flux by formula (33) and compare it with experimental DSC thermograms for three MGs. The characteristic volume of an elementary transformation was taken equal to $V_c = \gamma\Omega$, where γ is a numerical coefficient and Ω is the volume per atom. The dimensionless ratio B/γ was interpreted as a fitting parameter. The corresponding example is shown in Fig. 24, which compares the results of calculations and experiments for samples of the $Zr_{46}Cu_{45}Al_7Ti_2$ MG in the original and relaxed (by means of preheating to $T > T_g$) states. As can be seen, the calculation reproduces the experimental data very well, testifying to the adequacy of the described thermodynamic approach. In particular, the disappearance of the exothermic reaction in relaxed samples is reproduced well. Similar results were also obtained for other MGs [106]. Since it can be expected that $V_c \approx \Omega$, the results obtained yield values of the shear susceptibility $B \approx 20$, which are very close to those mentioned in Section 5, found in the analysis in the IT.

It should be noted that the structure of formula (33) for the heat flux is similar to that of the corresponding expression (5) derived in the IT. In both cases, the kinetics of the thermal effect is determined by the derivatives of the shear modulus with respect to temperature. The difference between the forms of these derivatives is partly due to the fact that formula (5) is more general, since it describes not only structural relaxation but also crystallization, while formula (33) is only applicable

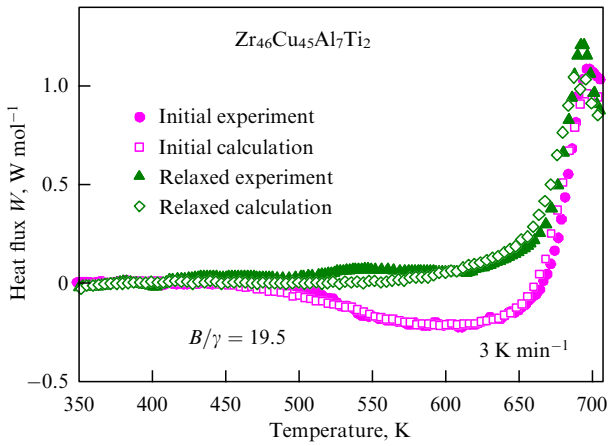

Figure 24. Heat fluxes calculated using Eqn (33) in comparison with experimental DSC thermograms for the $Zr_{46}Cu_{45}Al_7Ti_2$ MG in the initial and relaxed states [106]. Good agreement between the results of calculations and experiments is seen.

for structural relaxation. In the latter case, Eqns (5) and (33) yield virtually the same results.

We emphasize once again that the described approach to the kinetics of thermal phenomena based on general thermodynamic relation (30) is not connected in any way to the IT. However, the similarity of the obtained results indirectly confirms the adequacy of the analysis of thermal phenomena in the IT.

13. Problems and prospects

The consideration presented in this review shows that the IT makes it possible to describe, at least qualitatively, and in most cases, quantitatively, the main features of the relaxation behavior of MGs, in particular, the nature of the change in elastic and thermal properties during their heat treatment in various temperature regimes, including during crystallization. Despite the simplicity of the basic IT formulas that describe the physical properties of glass, it turns out that the dependences obtained on their basis reproduce the experimental observations well. This suggests that the concepts underlying the IT are universal. Moreover, although the IT was originally intended to describe glasses made of simple metals, it also quite adequately describes the behavior of multicomponent glasses. Thus, the IT is, on the one hand, relatively simple, and, on the other hand, a fairly effective tool for studying metallic glasses.

However, the IT itself requires further refinement and development. Granato's original version of the IT considered glass to be a comparatively homogeneous structure. However, the experimental and theoretical data presented in this review testify to the strong heterogeneity of the structure of metallic glasses, the properties of which, nevertheless, can be described using simple dependences. This poses some problems in IT refinement, as the complex nature of the structure is not apparently exhibited in the properties and behavior of the MG. One of the important areas in the further development of the IT should be the elucidation of the structure of glass based on simple metals. One of the problems is that the processes of clustering of interstitial dipoles and the resulting structures are relatively simply described only in the initial crystal structure. However, it is clear that the processes of dipole interaction highly depend on the nearest environment. So far, there is no adequate understanding of how the structure of a material evolves (even on the basis of simple crystal lattices) as the concentration of dipoles increases or how the nature and types of cluster formation change. Answering these questions may be one of the goals of computer modeling. Such studies can make a significant contribution to understanding the structure of glass.

Another area is connected with the study of multicomponent structures. As shown in Sections 4 and 10, one of the IT options is the representation of defects using the dipole model. However, examination based on the dipole model leads to virtually the same results as in the 'classical' IT. This is an important point that can be of great importance for understanding and studying multicomponent MGs. While in simple metals, in fact, the only variant of an effective elastic dipole is a split interstitial, in multicomponent crystalline materials, the number of variants of elastic dipoles is very large [21]. However, the role of such elastic dipoles both in the melting of multicomponent crystalline materials and in the formation of glasses based on them is still completely unclear. These two areas of studies may turn out to be key for the further development of the IT, on the one hand, and understanding the structure of glass, on the other.

It should also be noted that, as shown in this review, the IT well describes and predicts the behavior of the elastic and thermal characteristics of metallic glasses. However, so far, there are virtually no studies in which the IT would be used to describe other properties of MG, such as strength, plasticity, thermal conductivity, diffusion, or internal friction, with few exceptions [77, 107, 108]. The use of the IT to elucidate these properties will not only provide material for improving the theory itself and evaluating its adequacy but also deepen the understanding of structural features and relaxation phenomena in metallic glasses.

It also seems very important and interesting to use the IT to describe relaxation processes in nonmetallic (for example, oxide) glasses. The melting of the corresponding crystal structures differs significantly from that of metallic systems, and the existence of single interstitial dumbbells is far from apparent, although a wide variety of elastic dipoles can be expected. It is also of interest to use the IT to describe the properties of these materials. On the other hand, the structural diversity of nonmetallic glasses is inherent in systems that barely crystallize under standard heat treatment conditions, so the concept of a parent crystal loses its meaning for them. In general, the extent to which the IT can be applied to the description of nonmetallic noncrystalline systems is a matter for future research.

14. Conclusion

This review is devoted to an alternative view of the nature and properties of metallic glasses, the interstitialcy theory. This theory, first proposed about 30 years ago, has significantly developed only in recent years, taking its rightful place among the most promising approaches to the study of the nature, defect structure, and relaxation properties of metallic glasses. The fundamental feature of the interstitialcy theory is the presence of an organic connection between the properties of glass and the parent crystal from which the glass is made. Such a connection is embedded in the interstitialcy theory starting from the very first stage of formulating its basic hypotheses. In principle, it is this relationship that makes it possible to successfully interpret a fairly large range of

physical phenomena in metallic glasses, as shown in this review. In the opinion of the authors, with further development, this connection, along with the IT itself and the ideas embodied in it, may turn out to be useful for elucidating the structure and properties of nonmetallic noncrystalline systems.

Acknowledgments
This study was supported by the Russian Science Foundation (project no. 20-62-46003). The authors are grateful to colleagues A S Makarov, R A Konchakov, G V Afonin, E V Goncharova, and J C Qiao for the many years of fruitful cooperation.

References

1. Falk M L, Langer J S *Phys. Rev. E* **57** 7192 (1998)
2. Spaepen F *Scr. Mater.* **54** 363 (2006)
3. Miracle D B *Acta Mater.* **54** 4317 (2006)
4. Miracle D B et al. *MRS Bull.* **32** 629 (2007)
5. Cheng Y Q, Ma E *Prog. Mater. Sci.* **56** 379 (2011)
6. Egami T *Prog. Mater. Sci.* **56** 637 (2011)
7. Peng H L, Li M Z, Wang W H *Phys. Rev. Lett.* **106** 135503 (2011)
8. Wang D P et al. *J. Appl. Phys.* **114** 173505 (2013)
9. Zhang H et al. *J. Chem. Phys.* **142** 164506 (2015)
10. Fan H et al. *Mater. Horiz.* **8** 2359 (2021)
11. Richard D et al. *Phys. Rev. Lett.* **126** 015501 (2021)
12. Zanotto E D, Mauro J C *J. Non-Cryst. Solids* **471** 490 (2017)
13. Chen J, Zhao J, Cheng Y *Philos. Mag.* **100** 2938 (2020)
14. Granato A V *Phys. Rev. Lett.* **68** 974 (1992)
15. Granato A V *Eur. Phys. J. B* **87** 18 (2014)
16. Konchakov R A et al. *JETP Lett.* **109** 460 (2019); *Pis'ma Zh. Eksp. Teor. Fiz.* **109** 473 (2019)
17. Robrock K-H *Mechanical Relaxation of Interstitials in Irradiated Metals* (Berlin: Springer-Verlag, 1989)
18. Schilling W *J. Nucl. Mater.* **216** 45 (1994)
19. Wolfer W G, in *Comprehensive Nuclear Materials* (Ed. R J M Konings) Vol. 1 (Sect. Eds T R Allen, R E Stoller, S Yamanaka) (Amsterdam: Elsevier, 2012) pp. 1–45
20. Ma P-W, Dudarev S L *Phys. Rev. Mater.* **3** 043606 (2019)
21. Nowick A S, Berry B S *Anelastic Relaxation in Crystalline Solids* (Materials Science Ser., Vol. 1) (New York: Academic Press, 1972)
22. Holder J, Granato A V, Rehn L E *Phys. Rev. Lett.* **32** 1054 (1974)
23. Rehn L E et al. *Phys. Rev.* **10** 349 (1974)
24. Granato A V *Metall. Mater. Trans. A* **29** 1837 (1998)
25. Born M *J. Chem. Phys.* **7** 591 (1939)
26. Dederichs P H et al. *J. Nucl. Mater.* **69–70** 176 (1978)
27. Nordlund K, Averback R S *Phys. Rev. Lett.* **80** 4201 (1998)
28. Khonik V, Kobelev N *Metals* **9** 605 (2019)
29. Kobelev N P, Khonik V A *J. Exp. Theor. Phys.* **126** 340 (2018); *Zh. Eksp. Teor. Fiz.* **153** 409 (2018)
30. Gottstein G *Physical Foundations of Materials Science* (Berlin: Springer, 2004); Translated into Russian: *Fiziko-Khimicheskie Osnovy Materialovedeniya* (Moscow: BINOM. Laboratoriya Znanii, 2014)
31. Nordlund K et al. *Europhys. Lett.* **71** 625 (2005)
32. Konchakov R A et al. *JETP Lett.* **113** 345 (2021); *Pis'ma Zh. Eksp. Teor. Fiz.* **113** 341 (2021)
33. Kobelev N P, Khonik V A *J. Non-Cryst. Solids* **427** 184 (2015)
34. Makarov A S et al. *Intermetallics* **87** 1 (2017)
35. Safonova E V et al. *J. Phys. Condens. Matter* **28** 215401 (2016)
36. Goncharova E V et al. *JETP Lett.* **106** 35 (2017); *Pis'ma Zh. Eksp. Teor. Fiz.* **106** 39 (2017)
37. Gordon C A, Granato A V *Mater. Sci. Eng. A* **370** 83 (2004)
38. Granato A V *J. Non-Cryst. Solids* **307** 376 (2002)
39. Granato A V *J. Non-Cryst. Solids* **352** 4821 (2006)
40. Safonova E V et al. *JETP Lett.* **103** 765 (2016); *Pis'ma Zh. Eksp. Teor. Fiz.* **103** 861 (2016)
41. Zener C *J. Appl. Phys.* **22** 372 (1951)
42. Holder J, Granato A V *Phys. Rev.* **182** 729 (1969)
43. Dyre J C *Phys. Rev. B* **75** 092102 (2007)
44. Granato A V *Mater. Sci. Eng. A* **521–522** 6 (2009)
45. Kretova M A, Konchakov R A, Kobelev N P, Khonik V A *JETP Lett.* **111** 679 (2020); *Pis'ma Zh. Eksp. Teor. Fiz.* **111** 806 (2020)
46. Granato A V *J. Non-Cryst. Solids* **156–158** 402 (1993)
47. Donati C et al. *Phys. Rev. Lett.* **80** 2338 (1998)
48. Pazmiño Betancourt B A, Douglas J F, Starr F W *J. Chem. Phys.* **140** 204509 (2014)
49. Zhang H et al. *J. Chem. Phys.* **154** 084505 (2021)
50. Oligschleger C, Schober H R *Solid State Commun.* **93** 1031 (1995)
51. Oligschleger C, Shober H R *Phys. Rev. B* **59** 811 (1999)
52. Goncharova E V et al. *J. Phys. Condens. Matter* **29** 305701 (2017)
53. Brink T, Koch L, Albe K *Phys. Rev. B* **94** 224203 (2016)
54. Kobelev N P et al. *J. Appl. Phys.* **115** 033513 (2014)
55. Konchakov R A et al. *JETP Lett.* **115** 280 (2022); *Pis'ma Zh. Eksp. Teor. Fiz.* **115** 308 (2022)
56. Mitrofanov Y P et al. *Sci. Rep.* **6** 23026 (2016)
57. Khonik S V et al. *Phys. Rev. Lett.* **100** 065501 (2008)
58. Afonin G V et al. *J. Non-Cryst. Solids* **580** 121406 (2022)
59. Makarov A S et al. *Scr. Mater.* **168** 10 (2019)
60. Makarov A S et al. *J. Exp. Theor. Phys.* **134** 314 (2022); *Zh. Eksp. Teor. Fiz.* **161** 373 (2022)
61. Makarov A S et al. *J. Non-Cryst. Solids* **558** 120672 (2021)
62. Makarov A S et al. *J. Non-Cryst. Solids* **500** 129 (2018)
63. Mitrofanov Yu P et al. *Intermetallics* **101** 116 (2018)
64. Wang W H *Prog. Mater. Sci.* **57** 487 (2012)
65. Gordon C A, Granato A V, Simmons R O *J. Non-Cryst. Solids* **205–207** 216 (1996)
66. Goncharova E V et al. *J. Non-Cryst. Solids* **471** 396 (2017)
67. Makarov A S et al. *J. Non-Cryst. Solids* **521** 119474 (2019)
68. Makarov A S et al. *J. Phys. Condens. Matter* **32** 495701 (2020)
69. Mitrofanov Yu P, Kobelev N P, Khonik V A *J. Non-Cryst. Solids* **497** 48 (2018)
70. Nemilov S V *J. Non-Cryst. Solids* **353** 4613 (2007)
71. Angell C A *J. Phys. Chem. Solids* **49** 863 (1988)
72. Angell C A *J. Non-Cryst. Solids* **131–133** 13 (1991)
73. Angell C A *Science* **267** 1924 (1995)
74. Makarov A S et al. *J. Phys. Condens. Matter* **33** 275701 (2021)
75. Dyre J C *Rev. Mod. Phys.* **78** 953 (2006)
76. Dyre J C, Olsen N B, Christensen T *Phys. Rev. B* **53** 2171 (1996)
77. Granato A V, Khonik V A *Phys. Rev. Lett.* **93** 155502 (2004)
78. Nemilov S V *Glass Phys. Chem.* **21** 91 (1995)
79. Trachenko K, Brazhkin V V *Sci. Adv.* **6** eaba3747 (2020)
80. Sastry S *Nature* **409** 164 (2001)
81. Ohsaka K et al. *Appl. Phys. Lett.* **62** 2319 (1993)
82. Busch R, Liu W, Johnson W L *J. Appl. Phys.* **83** 4134 (1998)
83. Jiang H-R et al. *J. Alloys Compd.* **844** 156126 (2020)
84. Schawe J E K, Pogatscher S, Löffler J F *Thermochim. Acta* **685** 178518 (2020)
85. Makarov A S et al. *J. Phys. Condens. Matter* **33** 435701 (2021)
86. Makarov A S et al. *JETP Lett.* **115** 102 (2022); *Pis'ma Zh. Eksp. Teor. Fiz.* **115** 110 (2022)
87. Afonin G V et al. *Acta Mater.* **115** 204 (2016)
88. Phillips W A (Ed.) *Amorphous Solids*: *Low-Temperature Properties* (Topics in Current Physics, Vol. 24) (Berlin: Springer-Verlag, 1981)
89. Gil L et al. *Phys. Rev. Lett.* **70** 182 (1993)
90. Li Y et al. *Phys. Rev. B* **74** 052201 (2006)
91. Zorn R *Physics* **4** 44 (2011)
92. Mitrofanov Yu P et al. *Phys. Status Solidi RRL* **13** 1900046 (2019)
93. Makarov A et al. *Intermetallics* **141** 107422 (2022)
94. Vasiliev A N et al. *Phys. Rev. B* **80** 172102 (2009)
95. Granato A V *Physica B* **219–220** 270 (1996)
96. Khonik V A et al. *Phys. Status Solidi RRL* **12** 1700412 (2018)
97. Ingle K W, Perrin R C, Schober H R *J. Phys. F* **11** 1161 (1981)
98. Miracle D B, Greer A L, Kelton K F *J. Non-Cryst. Solids* **354** 4049 (2008)
99. Hirata A et al. *Science* **341** 376 (2013)
100. Zhu F et al. *Phys. Rev. Lett.* **119** 215501 (2017)
101. Konchakov R A et al. *J. Phys. Condens. Matter* **31** 385703 (2019)
102. Mitrofanov Yu P, Kobelev N P, Khonik V A *Phys. Solid State* **61** 962 (2019); *Fiz. Tverd. Tela* **61** 1040 (2019)
103. Makarov A S et al. *Intermetallics* **125** 106910 (2020)
104. Afonin G V et al. *Scr. Mater.* **166** 6 (2019)
105. Landau L D, Lifshitz E M *Statistical Physics* Pt. 1 (Oxford: Pergamon Press, 1980); Translated from Russian: *Statisticheskaya Fizika* Pt. 1 (Moscow: Nauka, 1976)
106. Makarov A S et al. *J. Phys. Condens. Matter* **34** 125701 (2022)
107. Qiao J C et al. *Prog. Mater. Sci.* **104** 250 (2019)
108. Yang D S et al. *J. Alloys Compd.* **887** 161392 (2021)